SANDIA REPORT

SAND2001-3996
Unlimited Distribution
Printed January 2002

Innovative Measurement Diagnostics for Analysis of Jet Interactions in Rotating Flowfields

Vincent A. Amatucci, Steven J. Beresh, John F. Henfling, Rocky J. Erven, and Chris J. Bourdon

Prepared by
Sandia National Laboratories
Albuquerque, New Mexico 87185 and Livermore, California 94550

Sandia is a multiprogram laboratory operated by Sandia Corporation, a Lockheed Martin Company, for the United States Department of Energy under Contract DE-AC04-94AL85000

Issued by Sandia National Laboratories, operated for the United States Department of Energy by Sandia Corporation.

Available to DOE and DOE contractors from
U.S. Department of Energy
Office of Scientific and Technical Information
P.O. Box 62
Oak Ridge, TN 37831

Telephone: (865)576-8401
Facsimile: (865)576-5782
E-Mail: reports@adonis.osti.gov
Online ordering: http://www.doe.gov/bridge

Available to the public from
U.S. Department of Commerce
National Technical Information Service
5285 Port Royal Rd
Springfield, VA 22161

Telephone: (800)553-6847
Facsimile: (703)605-6900
E-Mail: orders@ntis.fedworld.gov
Online order: http://www.ntis.gov/ordering.htm

SAND2001-3996
Unlimited Release
Printed January 2002

Innovative Measurement Diagnostics for Analysis of Jet Interactions in Rotating Flowfields

Vincent A. Amatucci, Steven J. Beresh, John F. Henfling, Rocky J. Erven,
and Chris J. Bourdon
Fluid, Thermal, and Aero Experimental Sciences Department

Sandia National Laboratories
P. O. Box 5800
Albuquerque, New Mexico 87185-0834

Abstract

The present document summarizes the experimental efforts of a three-year study funded under the Laboratory Directed Research and Development program of Sandia National Laboratories. The Innovative Diagnostics LDRD project was designed to develop new measurement capabilities to examine the interaction of a propulsive spin jet in a transonic freestream for a model in a wind tunnel. The project motivation was the type of jet/fin interactions commonly occurring during deployment of weapon systems. In particular, the two phenomena of interest were the interaction of the propulsive spin jet with the freestream in the vicinity of the nozzle and the impact of the spin rocket plume and its vortices on the downstream fins. The main thrust of the technical developments was to incorporate small-size, Lagrangian sensors for pressure and roll-rate on a scale model and include data acquisition, transmission, and power circuitry onboard. FY01 was the final year of the three-year LDRD project and the team accomplished much of the project goals including use of micron-scale pressure sensors, an onboard telemetry system for data acquisition and transfer, onboard jet exhaust, and roll-rate measurements. A new wind tunnel model was designed, fabricated, and tested for the program which incorporated the ability to house multiple MEMS-based pressure sensors, interchangeable vehicle fins with pressure instrumentation, an onboard multiple-channel telemetry data package, and a high-pressure jet exhaust simulating a spin rocket motor plume. Experiments were conducted for a variety of MEMS-based pressure sensors to determine performance and sensitivity in order to select pressure transducers for use. The data acquisition and analysis path was most successful by using multiple, 16-channel data processors with telemetry capability to a receiver outside the wind tunnel. The development of the various instrumentation paths led to the fabrication and installation of a new wind tunnel model for baseline non-rotating experiments to validate the durability of the technologies and techniques. The program successfully investigated a wide variety of instrumentation and experimental techniques and ended with basic experiments for a non-rotating model with jet-on with the onboard jets operating and both rotating and non-rotating model conditions.

Acknowledgements

The authors express their appreciation to the Laboratory Directed Research and Development Office of Sandia National Laboratories, managed by Charles E. Meyers, for its generous support of the Innovative Diagnostics LDRD research effort for a sustained period of three years. The LDRD Program is an excellent mechanism for high-risk and leading-edge research for the Laboratories and the funding was essential to the authors' diagnostics development plans and the advancement of our compressible flow research efforts within the Engineering Sciences Center.

In addition, the authors are grateful to managers Arthur C. Ratzel and Walter H. Rutledge of the Engineering Sciences Center for their enthusiastic support and interest in this program over the three years of its duration, and their dedication to fundamental experimental research in the aerosciences. These two managers have a history of strong investment in diagnostics development in the thermal, fluids, and aero sciences, and future validation experiments will succeed due to their support.

The authors also thank Carl W. Peterson and David W. Kuntz for their time, efforts, and expertise in reviewing this manuscript and making recommendations for changes. The excellent suggestions and technical insights from these two peer reviewers were instrumental in enhancing the quality of this report.

Table of Contents

List of Figures

1. Introduction

1.1 Problem Description

One of the long-term desires for experiments on subscale models in wind tunnels has been to fully instrument the model for onboard measurements. In particular, for problems characterized by complex fluid dynamic interactions both on the surface and in the vicinity of appendages, or characterized by rotation, it is often difficult to obtain measurements of flowfield properties relative to the vehicle in motion. In that case, it would be necessary to have diagnostics and instrumentation mounted onboard the model and thus obtain Lagrangian data in the reference frame of the model. This is true not only for measurements on subscale models in wind tunnels but also for flight test vehicles.

In the research program described herein, the primary goal was to determine whether an innovative class of instrumentation could be developed which would sense, acquire, and record pressure and rotation information on a model of the scale commonly used in Sandia National Laboratories' Trisonic Wind Tunnel (TWT) facility. The TWT facility is often used for force and moment measurements on bodies of revolution such as gravity bombs in an effort to assemble an aerodynamic performance model for guidance system applications. In these experiments the models are frequently less than 10% in scale and require the installation of a six-component force balance within the model. Getting additional instrumentation such as pressure sensors or imaging systems mounted in the model is extremely difficult when the models are so small.

The primary physical problem motivating an extensive set of research efforts is the case of a gravity bomb such as the B61 or B83 during the spin-up process immediately after aircraft release. In that instance, the vehicle is undergoing firing of the spin rocket motors for very short duration in order to impart a significant rotation rate to the vehicle.

1.2 Fluid Interactions and Effects on Vehicle Performance

As a consequence of the process of firing spin rocket motors on the B61 flight vehicle, powerful exhaust plumes exit from two scarfed nozzles slightly off-centerline of the bomb to impart spin rotation. This process is illustrated in the photograph included as Figure 1 for the B61-11 gravity bomb. The propulsive exhaust from a solid rocket motor injects a non-uniform supersonic stream into the transonic freestream for interaction both with the surrounding flow and also the downstream structures on the vehicle, namely the four fins. Since the strong transonic flowfield causes the two spin motor plumes to immediately bend and turn parallel to the vehicle longitudinal axis, their direct impingement on the fins as well as the effects of the vortices created by the plumes is important for study. It is the interaction of these flow

structures with the downstream fins and their effects upon the vehicle rotation rate that are of importance for understanding the flow physics of this problem.

Figure 1 Photograph of the B61-11 vehicle after release with spin rockets firing.

Since the B61 fins are slightly canted to the freestream flow to impart and sustain a rotation rate for the vehicle, any additions to their influence or negative effects upon torque need to be understood and predictable. In the B61 case, there is an overwhelming need for flowfield data from representative model experiments in wind tunnels for the same geometry and flow physics. In our case, that would require experiments and measurements in the TWT facility for a model geometry resembling the B61 gravity bomb and incorporating rotation.

The ultimate objective of the LDRD research project is to develop instrumentation capabilities and a model design that would, on a very small scale, represent the problem of a gravity bomb during the spin-up process. The focus of the three-year program was to develop pressure instrumentation based on MEMS technology, an onboard data acquisition and storage package, secondary jet capability, and optical diagnostics for measurements of flowfield properties on a 6% scale model located on a sting assembly in the one-foot square test section of the TWT facility.

1.3 Traditional Measurement Capabilities in Wind Tunnels and Flight Test

In traditional wind tunnel experiments, the major focus of data acquisition has been on forces and moments, which define the aerodynamic performance parameters of the vehicle. At times, there were arrays of body pressure measurements made, but in general the data was extracted from a six-component balance system mounted internal to the model along the longitudinal axis. The balance is normally located in the vicinity of the center of pressure of the vehicle and only a

handful of base pressure measurements were made to supplement the balance data. Flow visualization was usually limited to Schlieren imaging in the transonic and supersonic flows of the integrated flowfield features.

With the increasing demand for validation data for computational simulations, a wider range of data are needed to define and describe the flowfield at the surface of the model and in the near field. In particular, more extensive mapping of the pressure field is needed and density or velocity fields are highly desirable. In larger wind tunnel facilities external to Sandia National Laboratories, it is often possible to build large models which could house a larger amount of instrumentation, and often have a wide array of pressure and temperature sensors on the wind tunnel model. The extreme case of size is the flight test vehicle itself, which is by definition full-scale and thus able to sustain a large amount of instrumentation if project needs and funds allow. However, with both large-scale wind tunnel experiments and certainly flight test programs, the costs are often prohibitively high to acquire the type and extent of flowfield data needed for careful validation of computer simulations, or for basic flow-physics definition types of research projects.

Since both large-scale wind tunnels and flight test articles all rely on macro-scale instrumentation and diagnostics, the question arose whether the same type of information could be obtained by applying the newer technologies of micron-scale instrumentation and miniaturized data systems to achieve the same goals. Thus the idea was born for a diagnostics development research program which would attempt to apply the state-of-the-art in MEMS (MicroElectroMechanical System) devices and also miniaturized data acquisition, storage, and telemetry systems to analyze the flowfield on a rotating model in a small-scale wind tunnel.

1.4 Diagnostics Development and the Summary Report

During the course of this LDRD research program, there were parallel development efforts initially along four technology paths (outlined in greater detail in subsequent chapters of this document) aimed at obtaining quantitative data for a model in transonic flow with both plume exhausts and rotation. The utopian goal was a fully self-contained model and diagnostics that could actually present to the computationalist a surface and flowfield image of the pressure, velocity, and vorticity fields. While in reality this proved untenable at this stage of research, it should still be held as the ultimate experimental goal since, at least for the near future, small-scale experiments will always be an order of magnitude *less expensive* than using large-scale wind tunnels and *two orders of magnitude less costly* than flight tests.

The successes achieved during this LDRD research effort should be the first work towards a longer range goal of Lagrangian measurements in the TWT facility. Hopefully this will be achieved as diagnostics development and instrumentation miniaturization matures in the years ahead. Since complex geometries and flowfields seem to be more common for our weapons designs, there needs to be instrumentation and diagnostics developed which will provide sufficient measurements of the experimental flowfield for use by simulation efforts.

This final report summarizes developments and findings of the LDRD research program on innovative diagnostics for application to small-scale wind tunnels, in particular Sandia's TWT facility. While the majority of technical information on application of the technology to the wind tunnel experiments and experiences with the hardware are detailed in this report, full details (especially with regard to the hardware and software of the telemetry system and the quality and performance of the various microsensors) exist within the laboratory notes and publications of the authors, and the reader is referenced to them for further details, or to contact with the authors themselves. This research project and these experiments have only scratched the surface of possible wind tunnel applications of the TM hardware and software, and much promise lies ahead. The same is true for the application of micron-scale pressure transducers for wind tunnel research.

2. Program Background and Overview

This chapter presents a background description of the concepts behind the innovative diagnostics project and the technology basis that formed the belief in each of the capability development efforts. While the LDRD program on innovative diagnostics was successfully completed and achieved an informative investigation of the applicability of novel, miniaturized diagnostics for wind tunnels, the potential for extension of these findings to even more ambitious experiments is substantial. The history of the theory and experiences behind the LDRD experiments form a significant part of the learning process for this research program, and the value of the work as well.

2.1 Overview of Proposed Lagrangian Diagnostics

The advent in recent years of aerodynamic vehicles that combine complex geometries with rotation (for stability and dispersion minimization) has posed a difficult challenge for both modelers and experimentalists. The problem is characterized by three-dimensional interactions between the fluid and the vehicle structure, and *also* fluid/fluid interactions such as impingement of the spin rocket exhaust plumes on the freestream flow. Simulations of this rotating field are often difficult due to the inability of the flow solver to accept a rotating grid, and Lagrangian measurements on scale models are generally not performed due to the difficulties with placing sensors and data packages onboard the model.

The need for validation data and effective simulation tools for this type of rotating-body fluid dynamic problem is inevitable since they are *exactly* the type of aerodynamic vehicles under the design domain of Sandia National Laboratories. In particular, Sandia is presently poised, both computationally and experimentally, to take advantage of advances in technology to greatly advance the understanding of this problem. In the arena of experimentation, the development of micron-scale sensors, optical components, and lasers actually lays open the possibility of developing the measurement technology to acquire Lagrangian data for use in validating simulation tools. The information learned from this problem would also extend applicability of simulation tools to manufacturing processes characterized by rotating flow and all types of fluid flows in rotating machinery.

This LDRD research program was to develop innovative measurement instrumentation for acquiring qualitative and quantitative data in this complex spinning flowfield. The experimental setup would mimic the spin-up process for an air-dropped weapon, including modeling of the spin rocket exhaust plumes and their effects upon the freestream and the vehicle fins. The Lagrangian approach to data acquisition was (i) to measure surface pressures on the spinning model and (ii) to visualize the complex fluid interactions occurring on and near the surface of the spinning model – all with onboard instrumentation which do not bridge the structure upon which the model is spinning. The fundamental technical challenge is the fact that the model is small and

rotating. This would require either onboard storage of the data, or telemetering of the data to an off-model recording device.

The major technical issues were considered to be (i) packaging of the micron-scale instrumentation for use on a spinning model, (ii) storage and/or telemetry of the data on this scale, (iii) development of a MEMS-based optical system for flow visualization, and (iv) development of technology to deliver an onboard jet source for simulating the spin rocket exhaust plumes.

The illustration of Figure 2 shows a schematic of the concepts involved with the innovative diagnostics research program. All the elements needed for Lagrangian data acquisition are shown in Figure 2 as well as the difficulty with packaging of all of this instrumentation onboard a small-scale model.

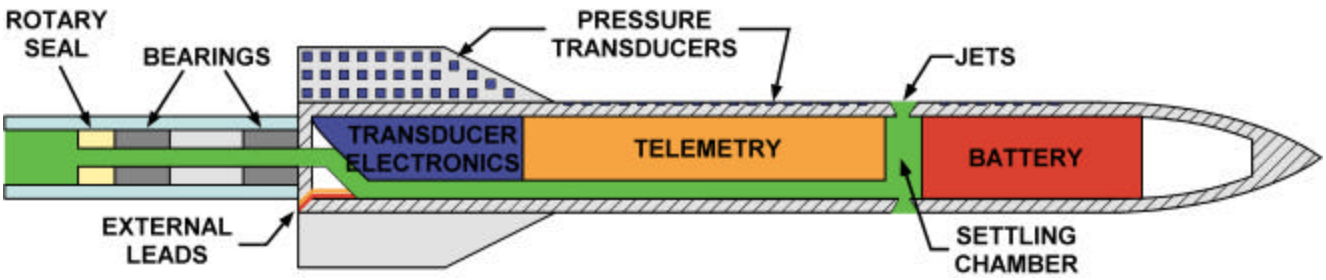

Figure 2 Schematic of the conceptual design of the innovative model.

The overriding approach of the research program was to piece together existing technology elements and to develop new capabilities and design/fabrication schemes to fill the gaps. In the Lagrangian frame of reference, the data would be used directly by simulation programs (both flowfield and trajectory) as they develop the spinning-grid capability in the existing aerodynamic flow solvers.

2.2 General Scales and Requirements for Wind Tunnel Models

Wind tunnel facilities and their respective models are usually divided into categories based on size and flight Mach number regimes. The cost of a program within a wind tunnel facility is usually directly proportional to the size of the model and generally increases with model design complexity. Although large facilities, and thus large models, afford the experimentalist the luxury of onboard instrumentation and data packages, they are usually "production" oriented in nature and less amenable to comprehensive validation experiments. In the early stages of this research program the possibility was examined to conduct the experiments external to Sandia National

Laboratories in a larger wind tunnel facility, but these ideas were discarded due to the high cost of external facilities and the LDRD budget constraints.

Thus, for applications within Sandia's TWT facility, the model would be kept to a scale below 10% and as near as possible to the 6-7% range commonly used. The model would also be sting-mounted for pitch and rotation control with new designs for minimal interference with the requirement to have a secondary jet delivered to the spin rocket nozzles. Normally, models within the foot-square test section of the TWT are kept to a diameter of 1.0 inch or less in order to keep the wind tunnel "blockage" below a few percent of the flow crossectional area. For the purposes of this LDRD research program, that constraint was eased slightly and the diameter range for the model was increased to between 1.25 to 1.5 inches if necessary. Since the experiments were aimed at being a "proof of concept" effort for onboard instrumentation, slight aberrations in the flowfield produced by a model slightly beyond our normal blockage constraints were acceptable. One luxury of the Mach number range of applicability (~M=0.8) for B61-type vehicles is that the influence of the near-field boundaries are relatively small. As the Mach number edges closer to 1.0, the influences become more dramatic.

Increasing the available diameter of the model, as well as locating the attachment plane at the aft end of the body instead of mid-body, would increase the volume available for onboard instrumentation. More insights into this capability will be detailed in Chapter 6 regarding design of the new wind tunnel model.

2.3 The Promise of Micron-Scale, MEMS-based Pressure Sensors

One key hope for many years in the Engineering Sciences Center was to determine the applicability of MEMS-based advances in sensor manufacturing to wind tunnel experiments on a small scale. Micron-scale sensors have shown great promise for applications such as automobile airbags (accelerometers) and *in situ* automobile engine and turbomachinery diagnostics (pressure and temperature transducers). Rapidly developing capabilities exist both within and outside of Sandia for design and fabrication of sensors on the micron scale [1-4]. The key difficulty has always been taking a sensor based on integrated circuit fabrication techniques and applying those sensors to wind tunnel type applications. In nearly all cases, the packaging poses the greatest challenge and technical performance of the sensor is a minor issue by comparison.

Prior to this LDRD research program, one of the authors gained experience with pressure and temperature sensors developed in the microelectronics facilities of Sandia National Laboratories. Those sensors, while performing reasonably well in terms of reliability, accuracy, and repeatability, demonstrated shortcomings with regard to both packaging and temperature sensitivity. Substantial shifts in the baseline signal for these devices occurred for even slight deviations in temperature, such as those occurring in a wind tunnel environment. The amount of signal noise varied greatly from sensor to sensor, even those manufactured in the same batch and on the same wafer. Thus, for the present LDRD program, the emphasis from the start was

to determine viable commercial vendors for micron-scale pressure transducers and then pursue acquisition of those sensors and installation as flush-mounted on the surface of the scale model.

While the world of micron-scale pressure sensors, and most MEMS devices for that matter, offers great promise of widespread application and massive arrays of transducers for complete spatial coverage, at present that technology is still in its infancy. The best application of those devices is one in which the sensor is effectively geometry-independent, such as the airbag sensor or general pressure sensing. For any applications to wind tunnel type flows, the greatest challenge to array-type products will be the ability to package them so that they are flush with the model surface (or in an ideal sense, integrated as part of the model surface) and tolerant of dynamic loads such as jet impingement upon the sensor surface.

The long-range vision for pressure sensor development on the micron scale is still the concept of a film of pressure sensors attached to conform to the model surface and containing literally hundreds or thousands of diaphragm-based sensors in a grid pattern. This would yield the type of continuous pressure field measurements perfect for use in comparisons with CFD predictions of the flowfield.

2.4 Plans and Direction for the Data Acquisition and Reduction Package

In the initial layout of the LDRD research program, the data acquisition and reduction package was modeled after traditional Sandia National Laboratories work with small models. Typically, the data package would consist of memory, processors, conditioners, amplifiers, and sensor attachments and would be self-contained within the test article. In most cases, however, the test article was still larger than our proposed geometry of the wind tunnel model for the TWT facility. Experience of the authors with both the micro-wet project (water projectile) and the Air Launched Raiding Craft experiments [5] guided the initial conceptual designs for data acquisition and reduction.

The data system for the LDRD model was intended and designed to accept a large number of sensor inputs from both the pressure transducers and the positional sensors. In the early concept schematics, the massive data from an onboard optical diagnostic was also intended to be sent to the data package for reduction and storage. In all cases, the “fallback” position was thought to be a Sandia-designed telemetry system for use in the TWT facility.

The data system was originally required to receive five channels of surface pressures from microsensors, two channels of base pressure data, two channels of shear stress sensor information, and five channels of “next generation” data (such as velocity, density, or temperature). The data system would incorporate multiplexing, signal conditioning, and either storage or telemetry of the signals via a “tell-tale” system interface. All of this information would then be transferred to a receiving station within the vicinity of the TWT facility.

The components of the data system were initially designed to be a combination of existing Sandia hardware from other small-scale data packages and further miniaturized boards specific to the LDRD needs. The plan was to expend some time and resources exploring the capabilities within Sandia before trying to find an external, specialty vendor for data packages.

2.5 The Challenges of Model Rotation for Jet Delivery and Data Transfer

Many of the technical aspects of onboard instrumentation for a model in the TWT facility are difficult before adding the complication of model rotation. Through the years, hardware such as slip rings have been used to transfer electronic signals across a moving boundary, but the transfer of a secondary gas stream was far more challenging. The usual apparatus used in the TWT for performing roll torque experiments with rotation involved a so-called "spin rig" which was essentially a taper-based mounting mechanism with roller bearings for relatively free rotation of the model. The hardware required for this sting-mounted rotation of the model utilized a significant amount of the internal volume of the already-small model and thus became a very undesirable methodology for mounting the LDRD model on the sting in the TWT facility.

The delivery of a secondary supply of gas to a small model in a wind tunnel is also a significant design challenge. Technical issues such as flow control, pressure/volume/time constraints, and nozzle modeling immediately come to mind for making the design non-trivial. The options of onboard storage of a volume of high-pressure gas versus off-board delivery of a gas stream must be weighed against each other. The mass of secondary gas needed onboard is simply defined by the pressure and flow rate of the spin rocket nozzles and the time duration for running the jets. In the present case, in order to obtain any amount of data, it was quickly determined that the nozzles would need to exhaust for a significant amount of time (essentially consistent with the running times of the TWT facility) averaging at least 30 seconds and sometimes longer in order to acquire the necessary pressure and rotation data.

Even with mass flow rate constraints handled, another important issue of plume modeling and plume matching need be considered. While the model design may emulate the scaled physical geometry of the spin rocket passages and nozzles, the fact that a different gas is being used for the simulation (i.e., different ratio of specific heats, γ), and at different dynamic pressure ratios, causes the experimentalist to examine and determine the influence of the variation in plume shape and effectiveness on the experimental data.

In the LDRD experiments, the simplest method to use for the proof-of-concept model was to match the scaled geometry of the spin rocket motors and then to extract information from existing literature regarding the effects of varying γ and dynamic pressure. The ability to suitably pass an adequate scaled mass flow rate would be a reasonable first step in examining the impingement properties of the two plumes.

2.6 Optical Diagnostics in an Ideal World

The optical diagnostics component of the LDRD project was conceptually very grandiose, and was subsequently shelved and deleted based on mid-year feedback of the LDRD review panel in the first year of the program. Long-range, however, the concepts layout the ultimate in a Lagrangian optical-based velocity diagnostic, and are worthy of some description.

As originally envisioned, the optical component of the LDRD project would have utilized the latest in state-of-the-art MEMS-based light sources, lenses, mirrors, and detectors to effectively build a visualization system onboard the model. Some of the technology exists [6-8] for design and fabrication of a laser-based optical system "on a chip" in microelectronic fabrication terms. The thinking at the start of this LDRD program was to build up a series of components which could be attached onboard the wind tunnel model and would produce a sheet of illumination in regions of interest in the spin rocket motor plume. The image of that illuminated sheet would then be captured by a miniaturized camera system and stored in the data package. The image would then be analyzed off-board the model for patterns in flow and general streamlines.

Taking the imaging system design one step further (certainly outside the bounds of the LDRD project in scope), with appropriate seeding one could take the next step and build up a *quantitative* velocity measurement system such as Laser Doppler Velocimetry [LDV] or Particle Image Velocimetry [PIV]. There are references in the literature for taking macro-scale laser systems and LDV measurement systems [9] and developing systems based on micron-scale technology and this should be implemented in the long-range picture for onboard acquisition of validation data for CFD simulations.

For the present, however, the LDRD review panel determined and suggested that the optical portion of the original proposal be dropped in favor of focusing the limited resources on the remaining technology challenges. Even sequencing of off-board image capture techniques to model position were considered and dropped as too difficult for the scope of the LDRD project.

2.7 The Realities and Limitations for Flowfield Diagnostics

The authors certainly acknowledge that the design and development of onboard measurement capabilities for a small-scale wind tunnel model are very challenging tasks for a wind tunnel as small as the TWT facility. However, one major objective has always been to move forward in the type of measurements offered to customers in the TWT facility, and in particular to determine better methodologies for providing pressure surveys on a model and data acquisition/transmission. Since larger wind tunnel facilities tend to offer their customers a wider range of onboard instrumentation, including extensive pressure data, angle of attack information, and even appendage force and moment data, the possibility for conducting these types of measurements in the TWT is worth some research.

The types of required aerodynamic data on models is expanding rapidly due to the demands of the CFD community, and small-scale wind tunnels will be the most challenged to accommodate these needs. Perhaps it is unrealistic to expect to acquire massive amounts of surface and flowfield data from 10% scale models with today's technology and sensors, but the boundaries of those capabilities must be explored. That is the primary product of this LDRD research program. In addition to the experimental data discussed and presented in Chapter 7, the "blind alleys" outlined in both Chapters 3 and 4 proved to be worthwhile endeavors and have also led to a better understanding of what can be accomplished in the TWT facility. The understanding of existing sensor and data technologies will both identify the gaps in capability and also determine the proper path for development of new approaches to measurements onboard small models.

3. Program Development and Design Approach

3.1 Validation Versus Benchmark Data Concepts

The initial plan for the three-year LDRD project was to develop a system of diagnostics which would, at the end of that three years, produce an experiment of "validation" quality. Thus goals were both the development of innovative diagnostics and the conduct of a validation experiment. As the work progressed in the initial year and discussions were held with the LDRD review panel, it became evident that the desire for "validation"-quality data was overly ambitious. Therefore, the LDRD program developed along the lines of a proof-of-concept project for diagnostics development ending with baseline "benchmark" experiments. These benchmark experiments would demonstrate the viability of the measurement system and not necessarily produce the well-documented, well-defined data sets needed for CFD validation comparisons.

Some concerns were raised regarding the use of micron-scale pressure transducers for acquisition of the pressure field on the surface of the model and the fins. While the transducers in the fins are miniaturized Kulite fast-response sensors, and demonstrate no issues with "quality of data," the MEMS-based transducers from common vendors are sometimes considered of lower quality for data acquisition due to their use of silicon for the pressure diaphragm instead of metal. The historical reliance of the wind tunnel community on macro-scale transducers with very precise fabrication and detailed calibration requirements drives these concerns regarding the micron-scale technology. The authors certainly acknowledge that the young stage of development for MEMS pressure sensors with typical 50 to 100μm diameter diaphragms is an issue that must be examined concerning level of accuracy of the data obtained.

In addition, the current project would address the measurement of certain quantities necessary for comparison with CFD simulations, but would not be totally comprehensive in all the details of approaching flow, boundary layers, shear layers, and three-dimensional effects to serve as a "validation" capability. In the long term that may be the evolution of this technology, but at present the experiments and associated data serve more the role of benchmark data – showing general trends only. The aim of the present program is to focus on developing the instrumentation technologies necessary for future acquisition of validation data in the TWT facility.

3.2 Description of Sandia's Trisonic Wind Tunnel Facility – the TWT

Sandia National Laboratories operates the Trisonic Wind Tunnel (TWT) facility located in Building 865 of Area I for subsonic, transonic, and supersonic experiments for a wide variety of vehicles. Usually the TWT facility has been used for force and moment experiments on bomb and reentry vehicle geometries to gain data that define aerodynamic performance parameters for the flight control system.

The TWT facility is a blowdown-to-atmosphere facility that uses compressed air at high pressure to produce high-speed flow over a model mounted in the 12-inch square test section of the wind tunnel. The facility can produce subsonic and transonic flows in the test section by using a converging nozzle in conjunction with perforated test section walls. Supersonic streams are achieved by using any of the converging-diverging nozzle walls with solid test section walls. Thus, the Mach number range of the wind tunnel is from approximately 0.5 to 2.5 with a relatively wide range of Reynolds numbers.

The TWT facility utilizes compressed air at approximately 300 psia and ambient temperature with a relatively large storage volume – affording operating times of anywhere from a few seconds to as long as one minute depending on stagnation pressure level. For subsonic and transonic Mach number operations, the flow is controlled through a combination of stagnation pressure setpoint and location of the downstream choke. For supersonic operations, the flow Mach number is defined by the installed set of converging-diverging nozzle hardware and the mass flow rate (or dynamic pressure) is determined by setting of the stagnation pressure level.

The wind tunnel operates with an automatic control system to maintain the set stagnation pressure level, and control movement of the pitch sector (upon which the model is mounted). While roll orientation of models is normally set manually, all other tunnel and data acquisition procedures are done remotely from the wind tunnel control room.

The TWT facility can be characterized as a moderate size wind tunnel, oriented more towards research-type experiments but capable of production-type measurements for aerodynamic performance. The wind tunnel is operated by a crew of three: a project engineer, instrumentation and data systems technologist, and hardware/compressor systems technologist. A schematic drawing of the TWT facility and system operations is included here as Figure 3, with photographs of the wind tunnel shown in Figures 4-7.

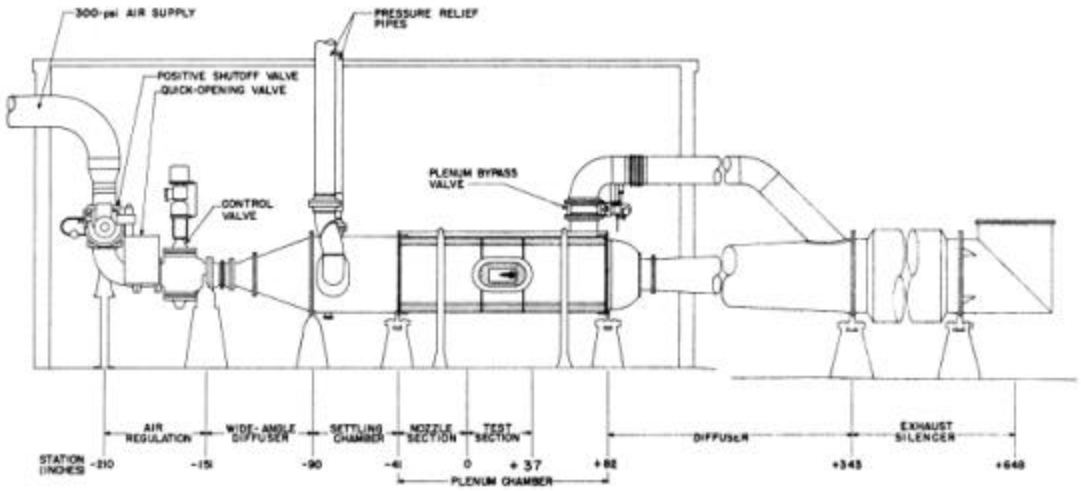

Figure 3 Schematic drawing of Sandia's Trisonic Wind Tunnel Facility.

Figure 4 An external view of the Engineering Sciences Experimental Facility.

Figure 5 An overview photograph of the TWT facility.

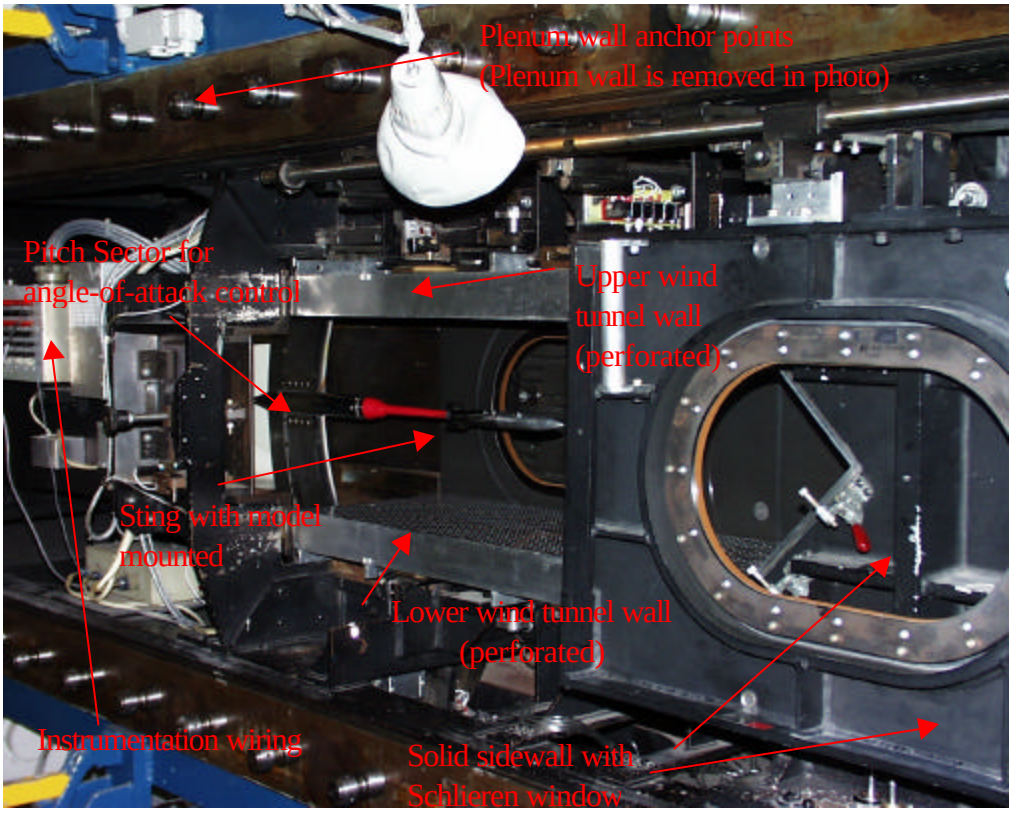

Figure 6 A photograph of the TWT facility with plenum sidewall removed.

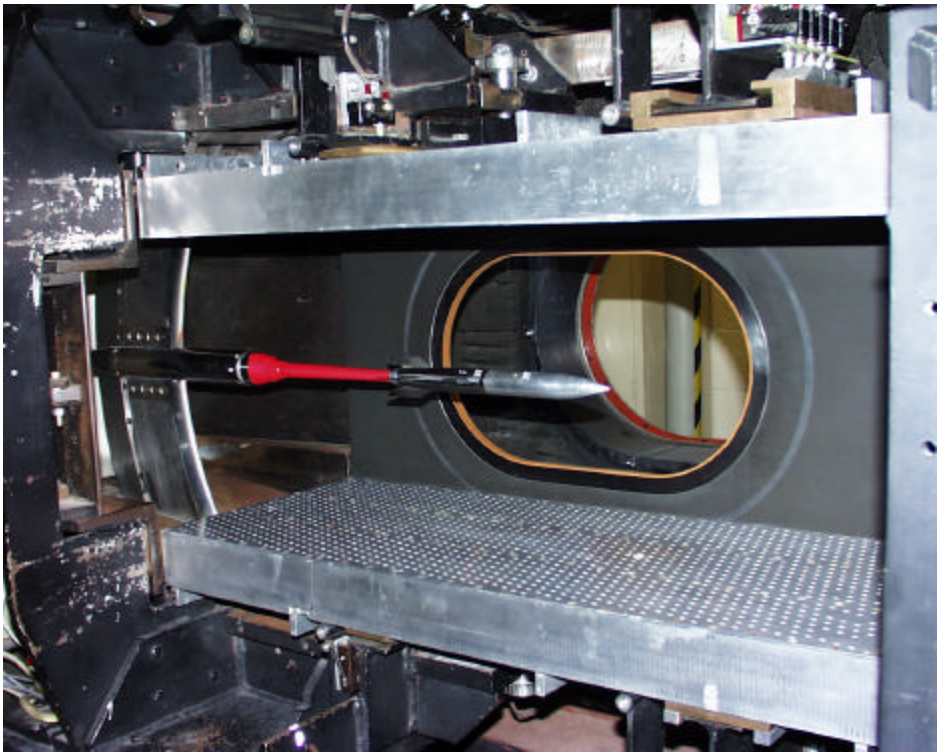

Figure 7 Photograph of the test section of the TWT illustrating model and sting.

3.3 Evolving Approaches

Early in the execution of the LDRD project, the fact emerged that this development effort was pushing back a number of significant boundaries for how experiments are conducted in the TWT facility. The most difficult challenge was the integration of techniques and capabilities which were well-proven with newer, modern ways of applying sensors and data packages. The program was thus consistently characterized by movement along paths which seemed promising, only to determine more efficient and cost-saving ways of achieving the goal.

In particular, as discussed in the sections to follow, data acquisition and sensor packaging tasks moved along very evolutionary paths, prior to finding a capability that worked well for application in the TWT facility.

4. Evolution of the Onboard Data Acquisition System

4.1 General Description of Data System Requirements

The specifications for the data acquisition and reduction system were outlined earlier in this report and were relatively modest for a data package. The original intent was to limit the number of data channels to less than approximately 16 since the first goal was to prove that a system could be packaged in the available volume. Thus, a blend of pressure and rotation rate data channels were selected for the first round, with the ability to expand later for other parameters such as pressure and temperature of the jet stagnation chamber, fin pressures, and eventual imaging data channels.

The path for development and design of the data acquisition and reduction package was to use expertise developed inhouse at Sandia National Laboratories and put together a miniaturized system to be self-contained within the wind tunnel model. In the past Sandia data systems experts have packaged the necessary acquisition boards, multiplexers, power circuitry, and sensor instrumentation for models as small as 2 or 3 inches in diameter and conical in shape. Thus, this seemed to be the best initial choice for data system development.

4.2 Data System Philosophy

Resources were invested in the first year of the LDRD project to allow David Armistead and Jeff Kalb of the Telemetry Technology Development Department to work on the data system design task. Their first approach, based on limited budget and the need for cost savings, was to determine whether existing hardware could be packaged in a new way to fit within the volume constraints of the wind tunnel model. Specifications were made for the number of data channels and transmission rates, but the small volume within the model proved to be the most difficult requirement.

After a reasonable amount of effort was expended on attempting to use Sandia data systems technology to attack this problem, a number of conclusions were drawn. First, no off-the-shelf components were available for use on the scale of the wind tunnel model. Second, only through a larger investment of funds and time *might* the data systems people successfully develop an onboard data storage system fitting within the volume of the defined model. And third, even if successful, the data storage system would only be able to accommodate a few channels of data. Thus, this effort proved to be not useful for the long term goals of the LDRD program.

Thus, relatively early in the LDRD project, the decision was made to discard the idea of data storage onboard the model and instead pursue the design/fabrication or acquisition of a data system which was capable of near-field telemetry of the acquired data. The system would still

need to be packaged within the volume constraints of the model but the potential for success was higher with this type of system. The best path for the telemetry system seemed to be to work with a number of commercial vendors who fabricated specialized telemetry systems mostly for automotive engine applications. Since the geometries with which they worked were quite unique, it was thought that our "unique" geometry would not prove exceedingly difficult.

The decision to telemeter the data from the rotating model was based on existing technology in 1999 and with the recent proliferation of small, personal electronics it would be interesting to revisit the data storage issue. This would be a worthwhile effort in a few years to determine if smaller memory chips and reduced-size power supplies might become available to do the job on a small item like the wind tunnel model.

4.3 Specialized Telemetry Systems

A thorough effort was conducted to research telemetry technology and to determine the types of systems that were available and how well-suited they might be to the application of the wind tunnel model. A number of commercial vendors were identified and the specifications of some of their custom-made systems were examined.

A promising path seemed to be working with Summation Research Incorporated (SRI) for design and development of a data TM system specific to the geometry of our model. The company makes a variety of one-channel and multiple-channel systems which are fairly standard in shape, but also performs custom fabrication of geometries to meet specific needs. In our case we were hoping for a multi-channel data unit with self-contained power and antenna.

The most appropriate system from SRI appeared to be the Series 400 units which combined 16 channel capability in relative small packaging. The Series 400 units leveraged cordless telephone technology to broadcast the data signals at 900 MHz and could be packaged on the small scale required in a shape consistent with the interior volume of the wind tunnel model. One unit from the Series 400 reads a maximum of 16 channels digitized at 8 or 12 bits and multiplexed across a total bandwidth of 25 kbps. The units also had the desirable feature of providing onboard an excitation voltage source for the pressure transducers, variable gain and offset for controlling the measured range of the transducer output, and a reasonably inexpensive rechargeable battery module.

The plan was to verify the flexibility and viability of the SRI hardware in an inexpensive way and then determine a design with multiple 16-channel units to meet our needs.

4.4 One-Channel Experiments with Modified Wind Tunnel Model

The first step in verifying SRI's technology was to acquire a one-channel system and become familiar with the hardware and software offered by the company. The single channel unit is illustrated in Figure 8 and clearly shows the advantage of small size and convenient packaging

offered by these SRI units. The single-channel unit consists of three modules: a processor, a transmitter, and (in this case) a disposable battery.

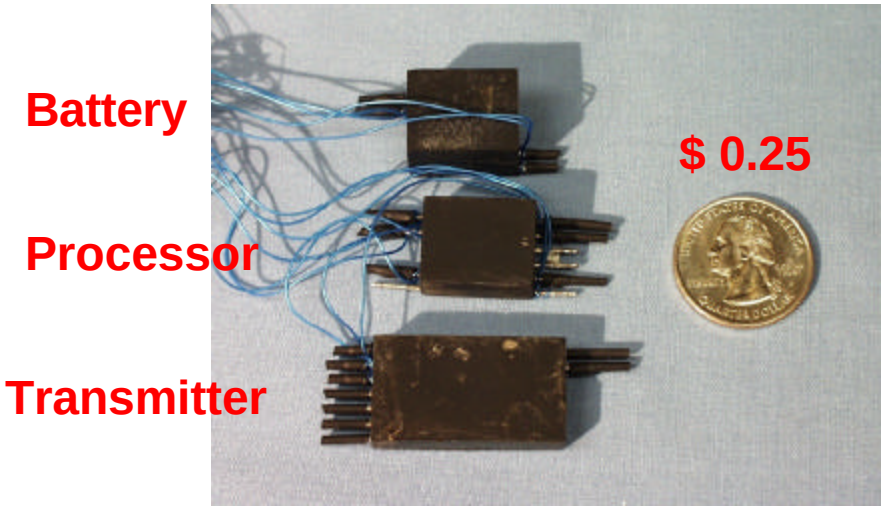

Figure 8 A photograph of the components of SRI's one-channel telemetry system

As part of the initial efforts to check out the single-channel TM data systems from SRI, it was necessary to find and modify an existing model used in the TWT facility. The goal was to find a model consisting of a gravity bomb-type exterior and a relatively large interior volume for packaging of the pieces shown in Figure 8.

The model shown in Figure 9 was selected and modified in size to accommodate the instrumentation, data system, and some rudimentary sensors. The model had an outside diameter of 1.25 inches and the internal cavity was only 0.75 inch diameter and approximately 6 inches long. A pressure tap was drilled into the model and a standard Kulite pressure transducer was installed to measure variations in pressure with angle of attack and rotation. To make sufficient room within the model for the telemetry hardware, the mounting location on the model was moved significantly rearward and the inner diameter was increased via machining.

While the hope was to minimize the changes to the external geometry due to the presence of the data system within the model, transmission from the unit was a concern. In the case of the one-channel system components, a small transmitting antenna protruded from the base of the model to provide a path for transmission of the acquired signal. The signal was thus clearly transmitted to the receiving unit located immediately outside the wind tunnel's plenum wall.

While these experiments were certainly not comprehensive or extensive, they did demonstrate the feasibility of the telemetry approach and verified that SRI's technology could accomplish the TM task within the TWT. As a demonstration data set, the signal from the Kulite pressure transducer was recorded during both rotating and non-rotating experiments and sent (via the TM system) to the receiver. The pressure signal was then reconstructed using the available D/A and A/D software and hardware provided by SRI.

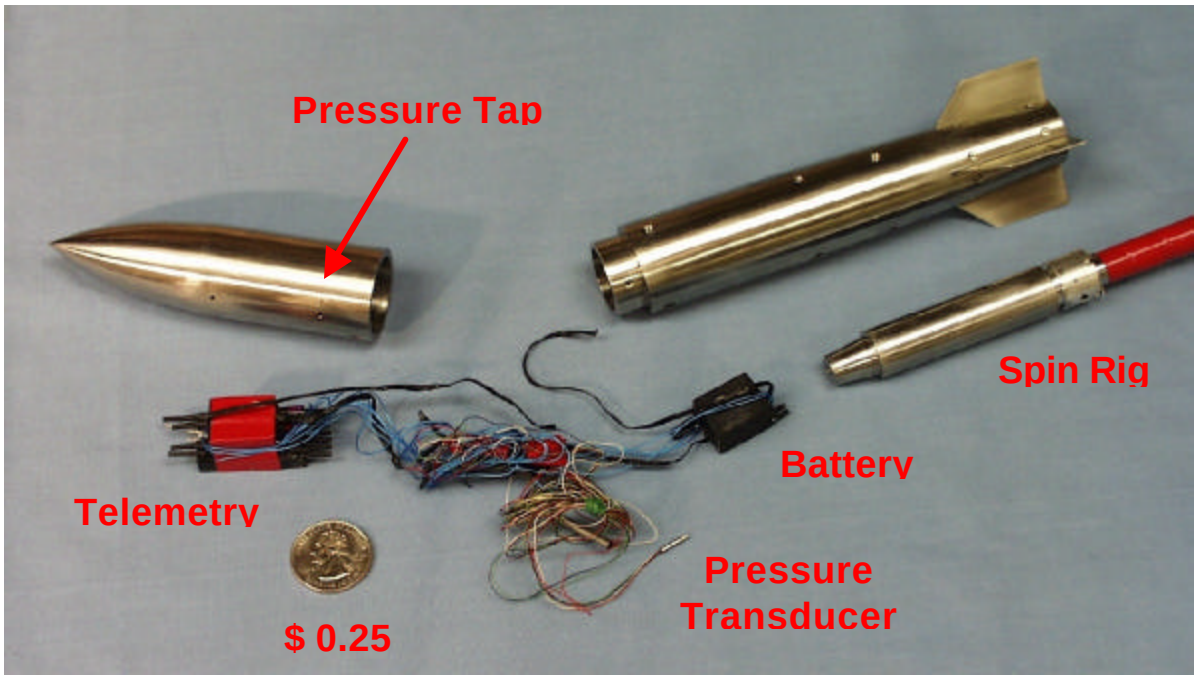

Figure 9 Photograph of the one-channel system and modified gravity bomb model.

As illustrated in Figure 10, the TM data system in conjunction with the Kulite pressure transducer produced the expected variations in pressure resulting from model rotation. Figure 10 shows the reconstructed pressure signal both in a phase-averaged sense and a sample instantaneous signal. In addition to the pressure variation from the windward to leeward sides of the model, the effects of model protrusions and imperfections also were visible in the data trends. The largest difficulty observed was a highly quantized nature to the data. This is attributable to fixed gain and 8-bit digitization, and can be addressed with the advanced unit using variable gain and offset capabilities and 12-bit digitization.

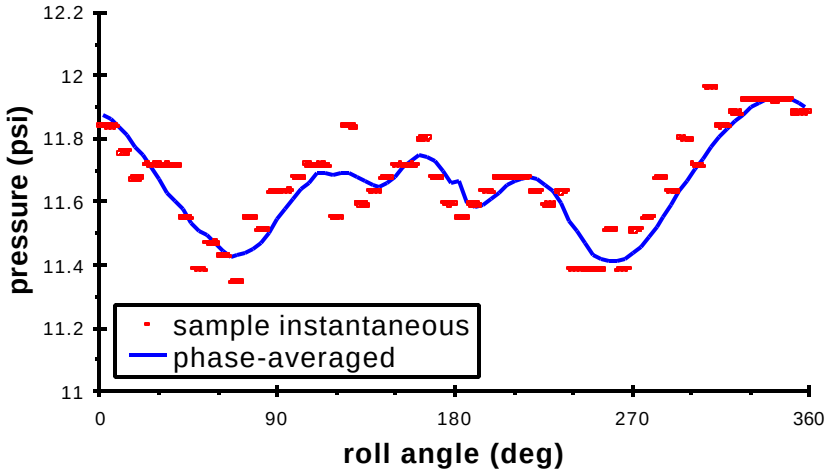

Figure 10 Pressure data, one-channel unit, M_8 = 0.8, P_0 = 16 psia, a = 20°, ?= 20 rev/s.

4.5 Multiple-Channel, Custom-Made Telemetry System

Based on the successful results of the experiments with the one-channel Series 300 telemetry system from SRI, confidence was gained to continue technology development efforts with SRI. The challenge was to specify requirements for the multi-channel transmitter/receivers and determine how many of the units could be packaged within our model. The 16-channel units were packaged as modified-cylinders and thus a number of them could be housed within the interior volume of the wind tunnel model.

The geometry for the transmitter and battery modules was specified as follows. The transmitters were to be housed within a 0.75 inch diameter with one side flattened by 0.15 inch for a length of 2.25 inches. The battery maintained the same cross-section as the transmitter modules but was 3 inches long. Figure 11 shows a photograph of one of the three identical transmitters compared to the size of a typical quarter dollar.

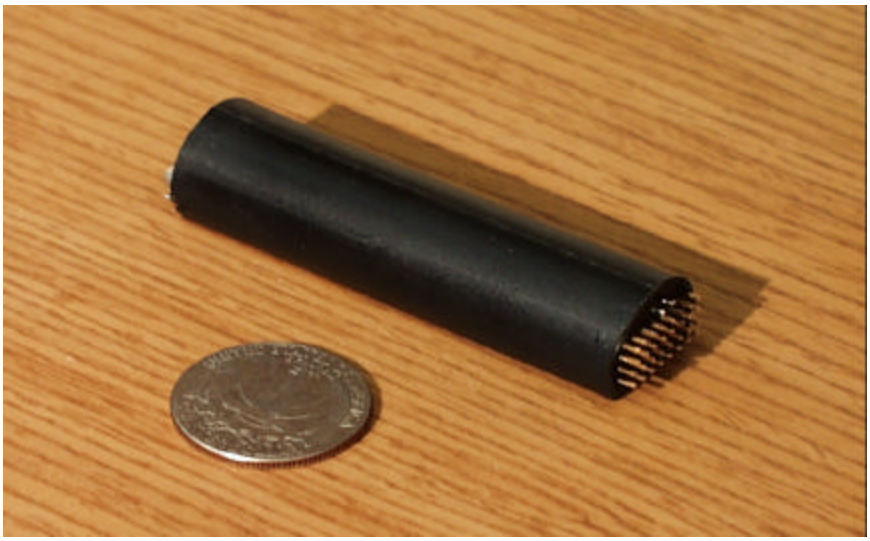

Figure 11 Photograph of the 16-channel transmitter module of the Series 400 unit.

The flattened side of the transmitter module reduces the minimum thickness of the unit to 0.60 inch in one direction, thus providing some room within the model to run instrumentation wiring or for installing a second transmitter module back-to-back. The reasoning behind this particular choice of crossectional geometry will become apparent in the discussion to follow for the design of the new wind tunnel model. Three Series 420 transmitters, three receivers, and one battery were purchased in an effort to provide a maximum of 48 channels of data for use at any one time. By changing the programmable configuration one could produce compromises between the number of channels, data bit depth, and sampling frequency appropriate to the experiments and to the instrumentation installed within the model. Some experiments might require the use of a maximum number of channels at a maximum accuracy, while others might prefer fewer channels and a more rapid sampling of data.

Another significant achievement made during the examination of the single-channel transmitter was the use of the spin rig to determine position rather than just angular velocity and acceleration. Historically, the Hall effect sensor has been used only for this limited role, but in the present experiments it was necessary to know the instantaneous roll angle at each point the pressure data were sampled. It was in this data collection mode that a phase-averaged representation of the pressure measurements could be assembled. This was accomplished by sampling the Hall effect sensor data in a different manner and implementing an algorithm to interpolate the Hall effect between the magnets found on the sensor to get a more accurate indication of rotational position prior to pressure signal sampling.

5. Micron-Scale Pressure Sensors and Instrumentation

5.1 Fundamental Performance of MEMS-based Pressure Sensors

The MEMS-based micron-scale pressure sensors were intended to be installed at a large number of positions on the model and initially also on one of the model's four aft-end fins. A good number of commercial vendors exist for pressure instrumentation and the technology is evolving in such a way that more and more "flush-mounted" sensors are becoming available. The goal of this LDRD project was to demonstrate that an array of pressure sensors could be installed along the length of the model and on the fin to provide a reasonable number of pressure data points for comparison with the CFD simulation predictions.

The vendors selected for study of their pressure sensor products were Motorola (Arizona), SenSym (California), and Lucas NovaSensor (California). In all cases, the goal was to identify and acquire piezoresistive-based sensors fabricated preferably by bulk or surface micromachining techniques. The available pressure microsensors were examined for a reasonable combination of onboard signal processing, low cost, and good sensitivity (and relatively good temperature insensitivity). In addition to these vendors of micron-scale transducers, investigations were also made for small-size pressure measurement systems from the Kulite company, a standard in the sensor business for wind tunnel measurement systems.

5.2 Selection of Sensor Vendors and Applicability to Model Measurements

Two specific types of pressure transducers were chosen for use in the customized wind tunnel model. One transducer is manufactured by Kulite Semiconductor and has been a staple of wind tunnel experimentation for many years. It is a piezoelectric transducer and is available packaged in a cylindrical design with a diameter as small as 0.063 inch. A more recent development is a similar piezoelectric design by Lucas NovaSensor and is packaged in a MO-8 surface mount microchip as the NPP 301 model. These two transducers are shown in Figure 12 and are compared with a Statham pressure transducer, which is a traditional aerospace sensor. The small size of the piezoelectric transducers as compared with the Statham sensor is evident.

Similar accuracy, sensitivity, and repeatability characteristics are displayed by all three transducers for consideration for these experiments. Clearly, the Statham transducer is simply too large for installation into a model which fits in the TWT facility. The Kulite and NovaSensor each have their own advantages with respect to one another. The slender cylindrical design of the Kulite transducer enables multiple transducers to be placed closer together to improve spatial resolution and gather more data, but it will protrude further into the interior of a wind tunnel model and thus interfere with the

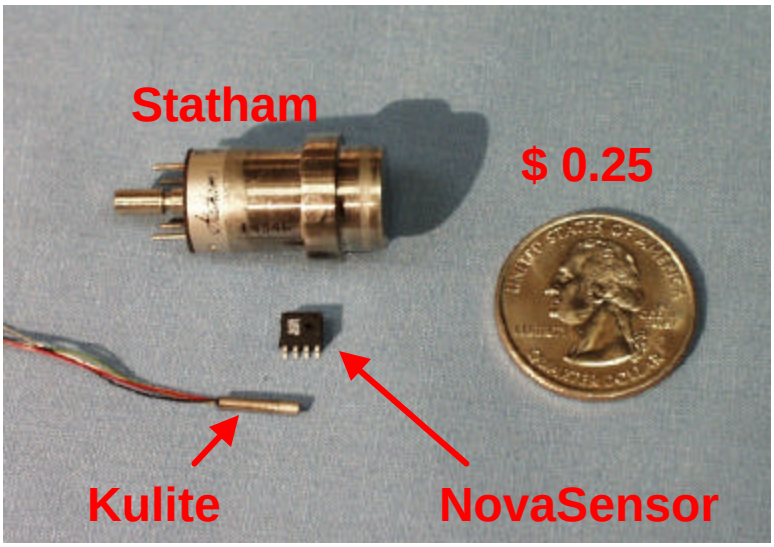

Figure 12 Photograph of pressure transducers showing relative sizes.

placement of the telemetry units and battery which must fit in the interior as well. Conversely, the NovaSensor transducer has a lower profile and will therefore provide more space for the telemetry transmitter modules and battery, but unfortunately the NovaSensor transducers cannot be spaced as closely and thus one returns to very discrete data in a spatial sense. The NovaSensor transducer also uses only 20% as much power the Kulite transducer at the same excitation voltage, which is an important advantage for a self-contained battery-powered model. Finally, the NovaSensor transducers are much cheaper than the Kulite transducers, costing approximately $10 each as compared to about $700 each.

An additional advantage for the Kulite transducers is that they are available as sealed-gage models, whereas the NovaSensor transducers are only available as absolute pressure transducers, thus somewhat limiting the applications range for the NovaSensor transducers. The "absolute" nature of the micromachined NovaSensor transducer is a direct artifact of the ability with the multi-layer fabrication process to enclose a chamber on the backside of the pressure diaphragm which is held at vacuum. Kulite transducers may be purchased that are sealed against atmospheric pressure and have a smaller pressure range, which increases the sensitivity of the transducer for small fluctuations near atmospheric pressure. Since jet/fin interactions of the type of importance to this LDRD research program are believed to induce only a very small pressure differential on the vehicle and across the fins, this is an extremely important benefit for the Kulite transducers.

The most appropriate use of pressure transducers for this research program was to acquire and use the NovaSensor packaged transducers for measurement of pressures along the length of the model and in the region on the body of the model between the fins. The Kulite transducers are

the natural choice for use on the aft end fins of the model, where the pressure differential is small and the fin is relatively thin.

5.3 Sensor Qualities and Performance

For piezoelectric transducers such as those fabricated by Kulite and NovaSensor, the pressure reading is primarily a function of the change in electric resistence on the pressure diaphragm, but will also be a minor function of temperature. This undesirable effect can be removed by placing a temperature compensation module into the circuitry of the pressure transducer, which is essentially a network of resistors whose values are carefully chosen to nullify the temperature effect over some range of temperatures. The Kulite transducers are provided with a temperature compensation module by the manufacturer (which in part accounts for the added expense) but the NovaSensors are not. Thus a temperature compensation module for the NovaSensor transducer can be constructed by the end user if required by the application.

A significant disadvantage of the temperature compensation modules for the present application is that they require more space. Given the tightly-packed conditions expected within the small-scale wind tunnel model, this poses a very difficult challenge. If the temperature influence upon the measurement is small, it may be an acceptable compromise to accept minor errors due to this temperature effect and free some space within the model for the data system components and wiring. To examine this issue, one of each type of transducer model was placed inside a temperature-controlled pressure vessel and pressure calibrations were performed for several different temperatures. It was found that over a range of 29°C, the calibration of the Statham transducer shifted by only 0.4%, the Kulite transducer by only 0.5%, and the NovaSensor transducer (some as expected and proven by past experiments [8]) by 6.4%. The Statham transducer is less susceptible to temperature effects since it is *not* a piezoelectric design, while the Kulite transducer includes a temperature compensation module, accounting for the minimal temperature effects. The NovaSensor transducer, as expected, displays greater variation with temperature effects unless a temperature compensation circuit is constructed for it and installed.

The temperature effect, if uncompensated, will be apparent in two ways. First, a calibration of the transducers at a different ambient temperature than the temperature at which the model will be exposed in the wind tunnel will lead to a bias error. Secondly, a temperature difference during experiments induced by the flow physics will also influence the pressure readings. However, since the jet/fin interaction experiments are planned for subsonic compressible velocities (Mach 0.5 – 0.8), the temperature variations within the flowfield are expected to be relatively small. Isentropic temperature variations at these velocities are within about 35°C, although transonic shocks may cause larger variations. Depending upon the desired experimental conditions and the location of the measurements, the temperature error may be deemed acceptable and a temperature compensation module may not be necessary. This issue will be examined as part of the experimentation with the new innovative diagnostics wind tunnel scale-model.

5.4 Instrumentation Characteristics

Prior to placing the new model in the wind tunnel to collect data, the characteristics of the pressure transducers were examined. The two performance parameters of primary interest are the instrumentation uncertainty and the dynamic response.

One contributor to the instrumentation uncertainty is simply the repeatability of a measurement. In addition to the normal precision error of a pressure transducer, which is typically quoted conservatively as 0.25% of full scale, the present experimental configuration has issues arising from the telemetry system. Any drift in the gain and zero offset by the transmitter will create precision error, and if the battery voltage is not sufficiently stable, the excitation voltage provided to the transducers will vary hence so will the transducer output signal. To examine these possibilities, several calibrations were conducted over multiple days with the battery at different charge levels. It was found that all the calibrations were virtually identical, with the 95% confidence interval of the calibration slopes found to be about 0.2%. A similar series of calibrations was conducted at a later date with somewhat different characteristics of the telemetry system and the same uncertainty was measured. The zero offset was only slightly larger, but drift in the zero offset is typically removed during experimentation by subtracting out a baseline measured prior to every wind tunnel run. Note that since the calibrations are determined from data points measured over several seconds of time, these uncertainties do not capture any instantaneous noise in the signal.

Other contributors to the instrumentation uncertainty are present, considering the novel and unique design of the wind tunnel model. For any pressure measurement, leaks are a potential source of bias errors. While no leaks were detected during the model checkout phase, repeated re-assembly of the model and the additional stresses during a wind tunnel run may produce small leaks. Burrs or dirt located at a pressure tap are a well-known source of error, and given the small size of the pressure taps on the current model, pose a particular concern. Care was taken to keep the model surface as clean as possible and the surface and fin pressure taps free of debris accumulated during model assembly.

The dynamic response of the instrumentation is important because the pressures will vary as the model rotates. If the instrumentation cannot respond suitably fast, measurement variations will be averaged out to produce a value that is merely the mean pressure around the perimeter of the model as it rotates, thereby obscuring the very data this LDRD project was designed to generate. To characterize the dynamic response of the entire apparatus, including the pressure transducers, pressure taps, and the telemetry system, vacuum was applied to a particular pressure port and then abruptly removed. The response of the system was measured as the pressure increased from vacuum to atmospheric levels. This approximates applying a step function change to the instrumentation and provides a more extreme pressure change than what is likely to be seen during an actual wind tunnel experiment; therefore this offers a conservative examination of the dynamic response. Several tests were conducted in which the pressure rise to which the transducer was subjected was about 4 psi, a sample of which is shown in Figure

13. Also shown in the figure are dashed lines indicating the 10% and 90% pressure rises, the time between which is 2.05 ms. This value can be used as a characteristic rise time and hence a measure of the response time of the transducer coupled through the telemetry system. The speed at which the vacuum hose was removed from the pressure port is also a factor. Regardless, the 2.05 ms response time is a conservative measurement and the actual dynamic response can be no worse than this.

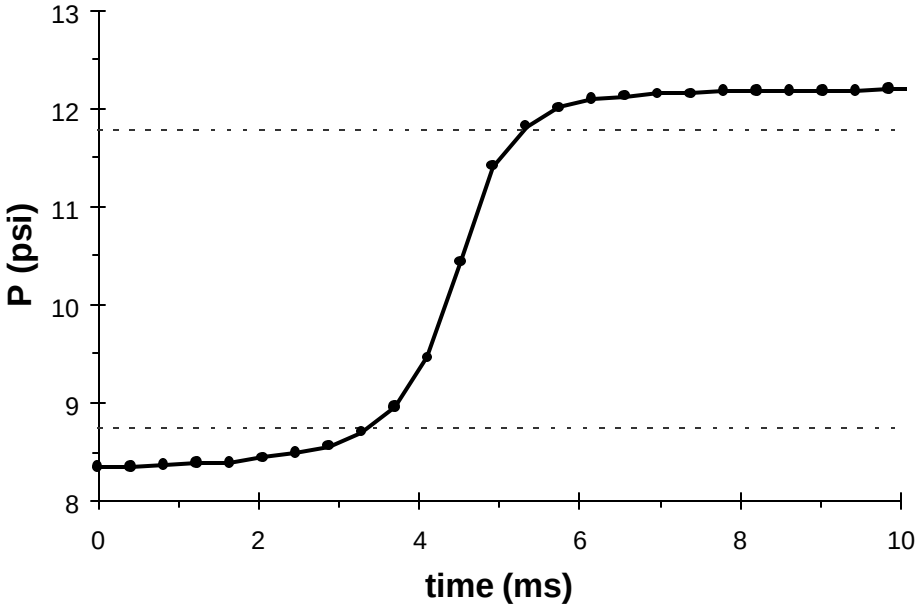

Figure 13 Pressure response of a NovaSensor transducer to a 4 psi step change. Dashed lines indicate the 10% and 90% pressures (2.05 ms rise time).

An additional issue to be considered is synchronization between the acquisition of onboard pressure data from the transducers and the offboard Hall effect sensor which provides model rotation and position data. The pressure signals from the transducers on the model are passed through processing electronics in both the telemetry transmitter and the receiver. This processing takes a finite amount of time. The Hall effect sensor, on the other hand, does not experience similar delays. To address this synchronization issue, a benchtop experiment was conducted in which a known wave produced by a function generator was passed through the telemetry system and examined in comparison to the original signal. The resulting delays are shown in Figure 14 for both 8- and 12-bit sampling and varying quantities of multiplexed channels.

The data in Figure 14 demonstrate that for a single channel the measured delay is 37.5 ms for 8-bit sampling and 34.5 ms for 12-bit sampling, with an uncertainty of 0.5 ms or less. As more channels are multiplexed, this delay and the uncertainty of the measurement rise because the beginning of the sampled waveform did not necessarily coincide with the first telemetered channel. The 12-bit delay rises at a faster rate for increasing quantity of channels because of the additional time required to telemeter the extra bits needed for each sample. The fundamental

delay through the transmitter is given by the single-channel measurement, with additional delays resulting simply from the time required to multiplex through more channels to reach the one of interest. During a wind tunnel experiment, acquisition of data from the Hall effect sensor will be initiated simultaneously with the acquisition of telemetered data beginning with the first channel. Therefore the single-channel delay shown in Figure 14 is the relevant value, with subsequent channels exhibiting additional delays based upon the sampling rate.

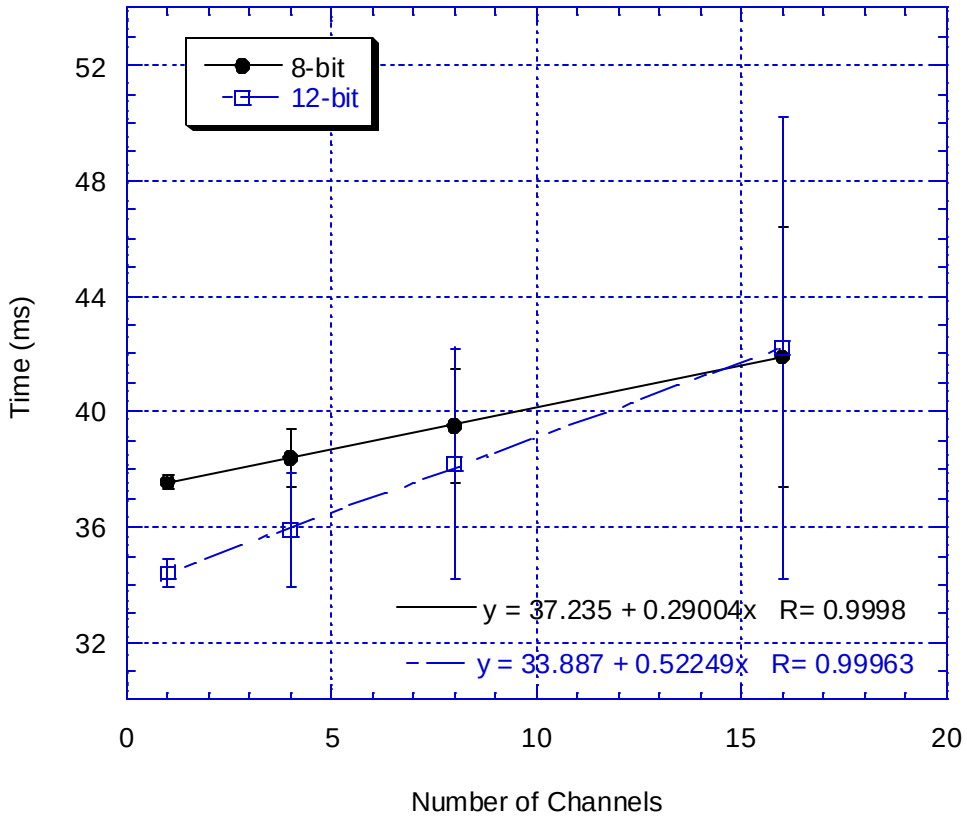

Figure 14 Telemetry system time delays transmitting a function generator signal.

6. Mechanical Design of the Wind Tunnel Model

6.1 General Requirements for the New Wind Tunnel Model

To accommodate the experimental goals of this LDRD project, it was necessary to design and fabricate a highly innovative wind tunnel model. Traditional models used in the TWT facility at Sandia are approximately 1 inch in diameter, about 8-10 inches long, and contain either an six-component force and moment balance or a spin rig within the center of the model. Because the present research program requires a much greater quantity of instrumentation to be placed within the model, the decision was made to design a slightly larger model of 1.5 inch diameter and 14 inches long. Furthermore, the mechanism for rotation of the small-scale model would be relocated to the rear of the model and attached directly to the sting. This single design feature would produce a much greater volume within the main body of the model for placement of sensors, the data package, batteries, and the associated wiring.

Other changes from the traditional model design for the TWT facility were intended to provide better access to the inside of the model for installation and maintenance of the instrumentation. One of these features included a modular model design so that portions of the model could be removed to gain unique access to instrumentation and wiring, including a "clamshell" design that split the model lengthwise down the middle.

In addition to providing measurements while the model is rotating, the new model also was intended to include the capability for a supply of a secondary gas to simulate the exhaust plumes of spin rockets used for initial roll control of gravity bombs. The simulation of the spin rocket jet exhausts requires a high-pressure gas source to supply the settling chamber feeding the two nozzles. Initial consideration was given to using a small compressed gas source on the model, but there would be insufficient space to hold a meaningful supply of gas in addition to the regulator that would be required in the model to maintain a constant pressure (and thus mass flow rate) for the jets. Instead, a better approach would be to pass the gas across a rotating junction in the spin rig to supply the jet nozzles installed in the model and thus allow gas pressure and flow rate regulation to be accomplished exterior to the model.

6.2 Basic Model Design

Conceptual drawings of the new wind tunnel model are included in Figures 15 through 18 and give an overview of the internal and external features of the unique design. The actual drawings that were used for model fabrication are too extensive and complex to represent and include here in this report, but are available directly from the authors upon request. The new wind tunnel model was designed to be a generic finned axisymmetric body with the dimensions outlined in Figure 15.

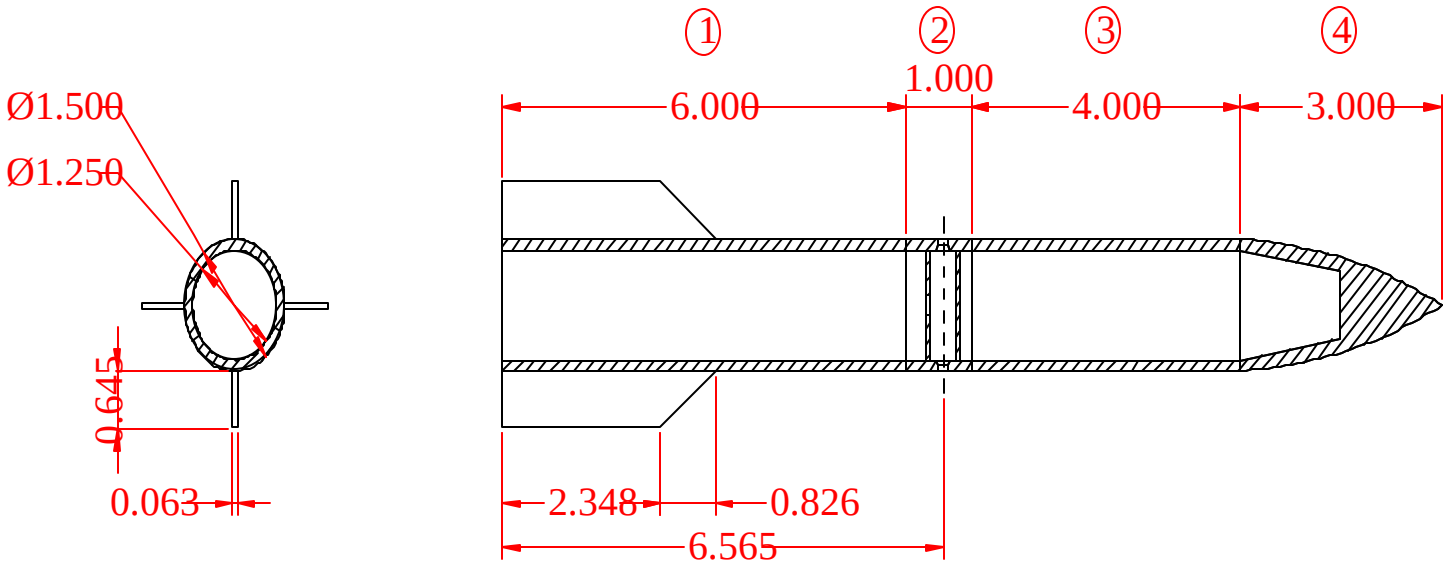

Figure 15 Assembly view and basic dimensions of the new wind tunnel model. (Image slightly distorted to fit onto page)

The model separates into four distinct axisymmetric segments, labeled 1 through 4. The two largest segments, 1 and 3, open longitudinally into two parts to maximize access to the inside for instrumentation. A dovetailed rail joins the longitudinal sections, which are threaded at their ands and clamped together by the adjacent segment. The overall length of the body is 14 inches with an outer diameter of 1.5 inches and an inner diameter of 1.25 inches. Conceptual drawings of model segments 1 and 2 are shown in Figures 16 and 17. The design of segment 3 is easily extrapolated from segment 1 and segment 4 is simply an ogive cylindrical nose with a hollowed interior.

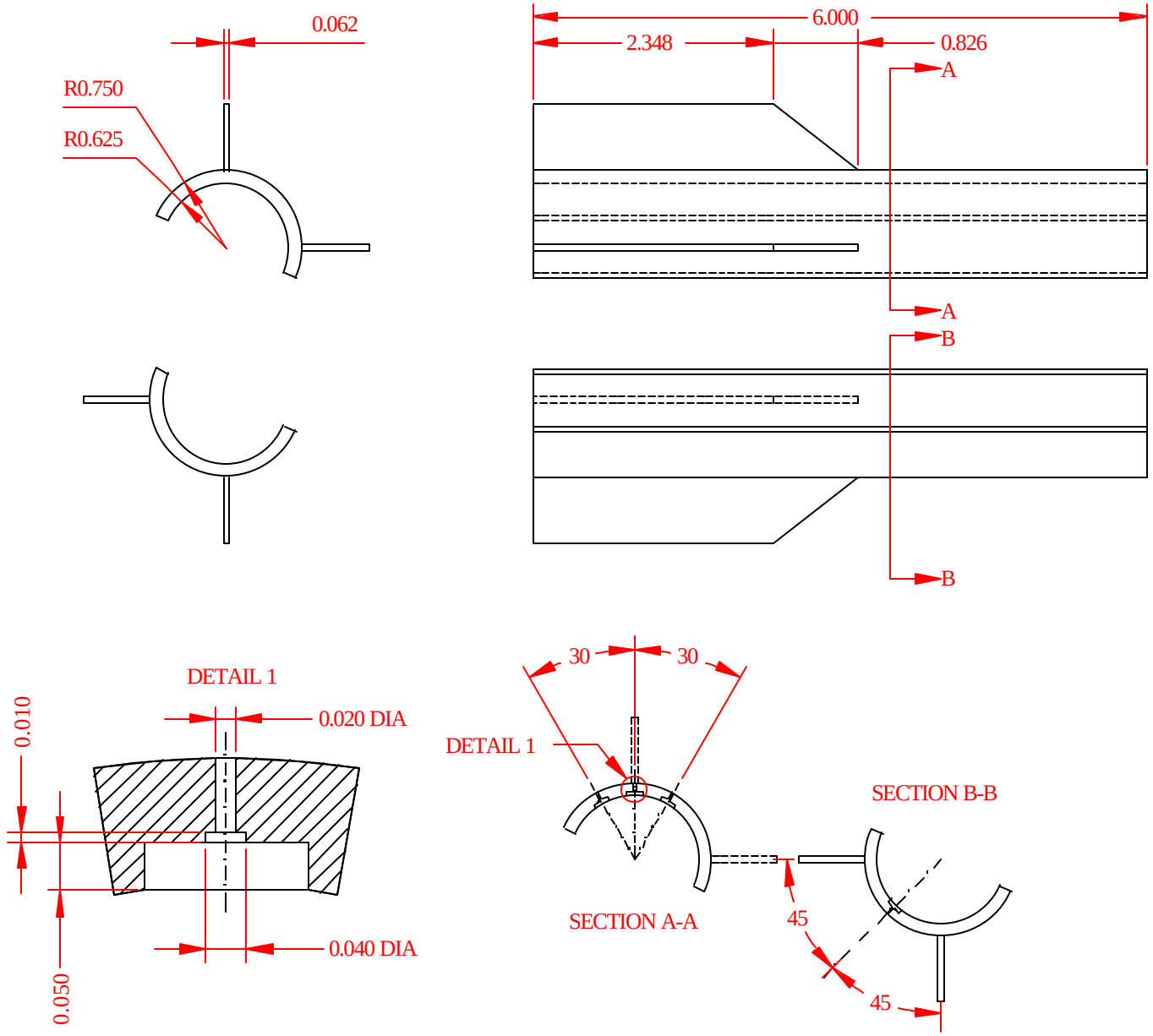

Figure 16 Conceptual drawing of Segment 1 of the model; Segment 3 is analogous.

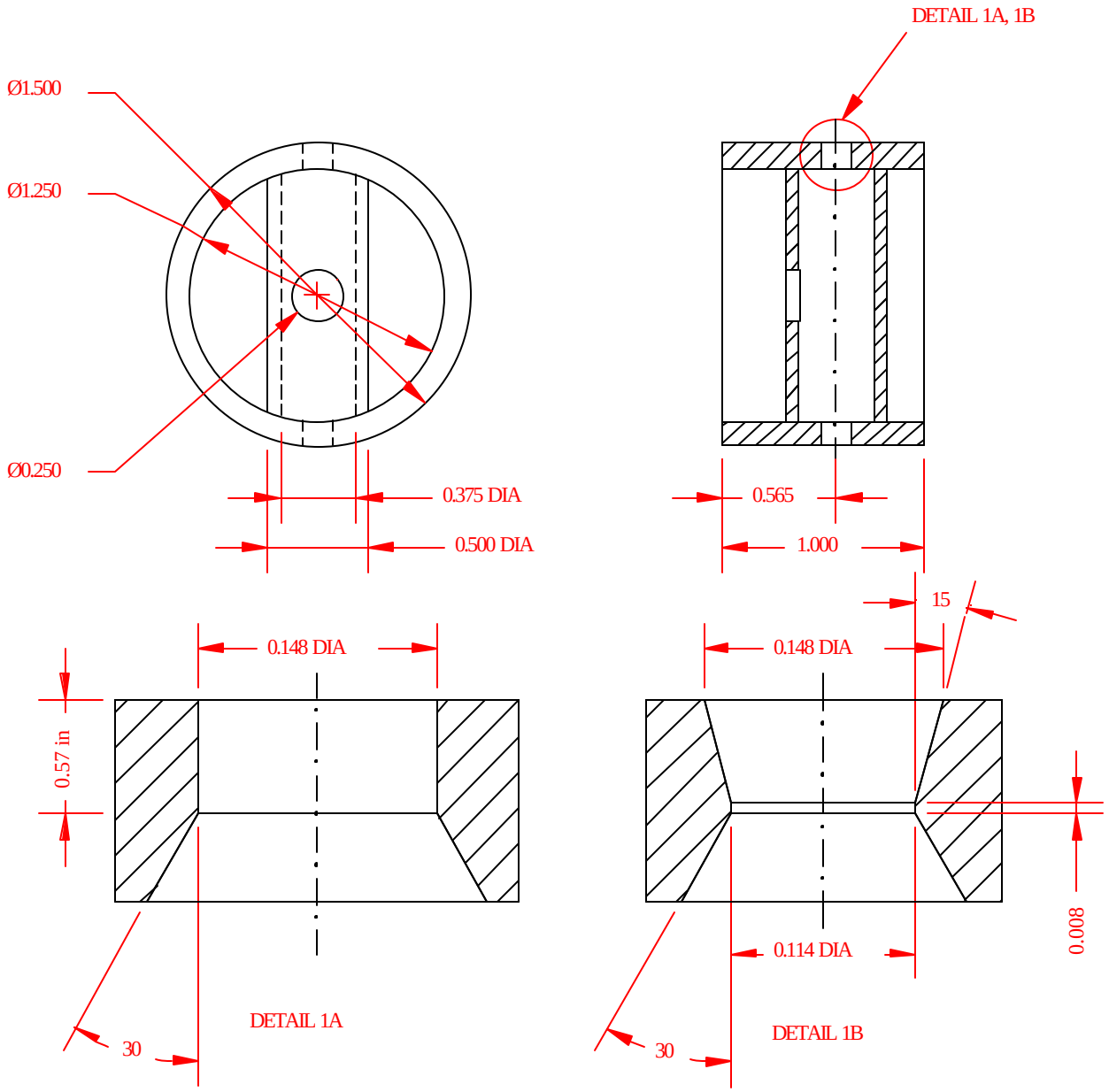

Figure 17 Conceptual drawing of Segment 2 of the model, including two of the three alternative details; the missing detail is simply a solid wall.

Model segments 1 and 3, which are the fore and aft segments of the model, respectively, contain many mounting points for the micron-scale pressure transducers manufactured by NovaSensor. As illustrated in Figure 16 for Segment 1 (Segment 3 is analogous), a recessed flat is machined into the cylindrical inner contour of the model to allow placement of the pressure transducer flush-mounted to the drilled pressure tap. The segment opens lengthwise into two

separate pieces for easy instrumentation access for both installation of the NovaSensor pressure transducers and the soldering, connecting, and running of wiring. One half of the aft segment supports a row of transducers beginning at the fin root and extending forward, with an additional row 30 degrees to each side that runs the length of the model segment.

Section A-A of Figure 16 indicates this arrangement forward of the fin; a section taken through the fin would show only the two 30-degree rows of pressure transducers and not the central row. The other half of the aft segment contains a single row of pressure transducers extending its length, located 45 degrees from the fin as shown in Section B-B of Figure 16. In similar fashion, the fore segment opens lengthwise into two separate pieces and one of the two halves contains a single row of transducers extending the length of the model segment. All transducer rows possess a spatial resolution of four transducers per inch. While this provides 92 transducer mounting locations for the entire model, all transducer locations are not intended to be used simultaneously; rather, different subsets of locations will be employed for different experiments based on need.

A cross-section of the pressure transducer mounting surface is shown in Detail 1 of Figure 16. A pressure tap of 0.020 inch diameter connects to a cavity 0.040 inch in diameter, which fits over the 0.030 diameter orifice of the NovaSensor pressure transducer. A rectangular cavity is machined to hold the transducer itself, with dimensions slightly larger than the transducer to allow for epoxy to both secure the transducer in place and to seal the cavity. A Kulite transducer may be mounted into any pocket by using a dummy transducer shaped like a NovaSensor, then epoxying the Kulite into a hole in the dummy transducer.

The fins shown in the aft segment are actually removable from the body. This allows different fin sets to be installed onto the wind tunnel model for different experiments. This feature is aimed at addressing the eventual need to examine the effects of jet/fin interaction for a wide range of fin cant angles. Fin cant angle values have been selected to rotate the model at no more than 10 Hz. Simple slab fins were used rather than a complex fin geometry since first order proof-of-concept was the simple goal for the LDRD project. In addition, a single fin has been designed for installation of custom pressure instrumentation by Kulite, where miniature transducers will be flush-mounted directly in the 0.063 inch thick fin. Channels of 0.020 inch depth were milled into positions on each side of the fin, which was sent to Kulite for customized packaging of the pressure transducers. The need for sufficient fin depth for this instrumentation was an additional reason for the use of slab fins. The details of the instrumentation of this fin will be discussed in greater detail below.

The center segment of the model, which is segment 2 and is shown in Figure 17, is a short portion of the model containing a pair of nozzles used to simulate the spin rocket exhaust jets. As with the use of removable fins to attain different fin cants, the center segment is interchangeable to allow different geometries to be studied for the exhaust jets. Details 1A and 1B show two of these, representing a sonic nozzle and a Mach 2 nozzle. A third version contains no jets or settling chamber and instead acts simply as a hollow section for experiments where jets are not required. The settling chamber for the jets is supplied by a tube leading from

the rear of the model through the center segment. The settling chamber does not occupy the entire cross-section, because space is needed to pass wiring between the fore and aft segments for all of the pressure instrumentation installed in the wind tunnel model.

6.3 Special Features of the Wind Tunnel Model

Figure 18 shows the assembly of the model with the telemetry apparatus and the pressurized gas line in place. A cross-section also is shown to indicate how three transmitters and one battery can be made to fit within the model even with the gas line and transducers in place. Open spaces are used to pass the large volume of wiring.

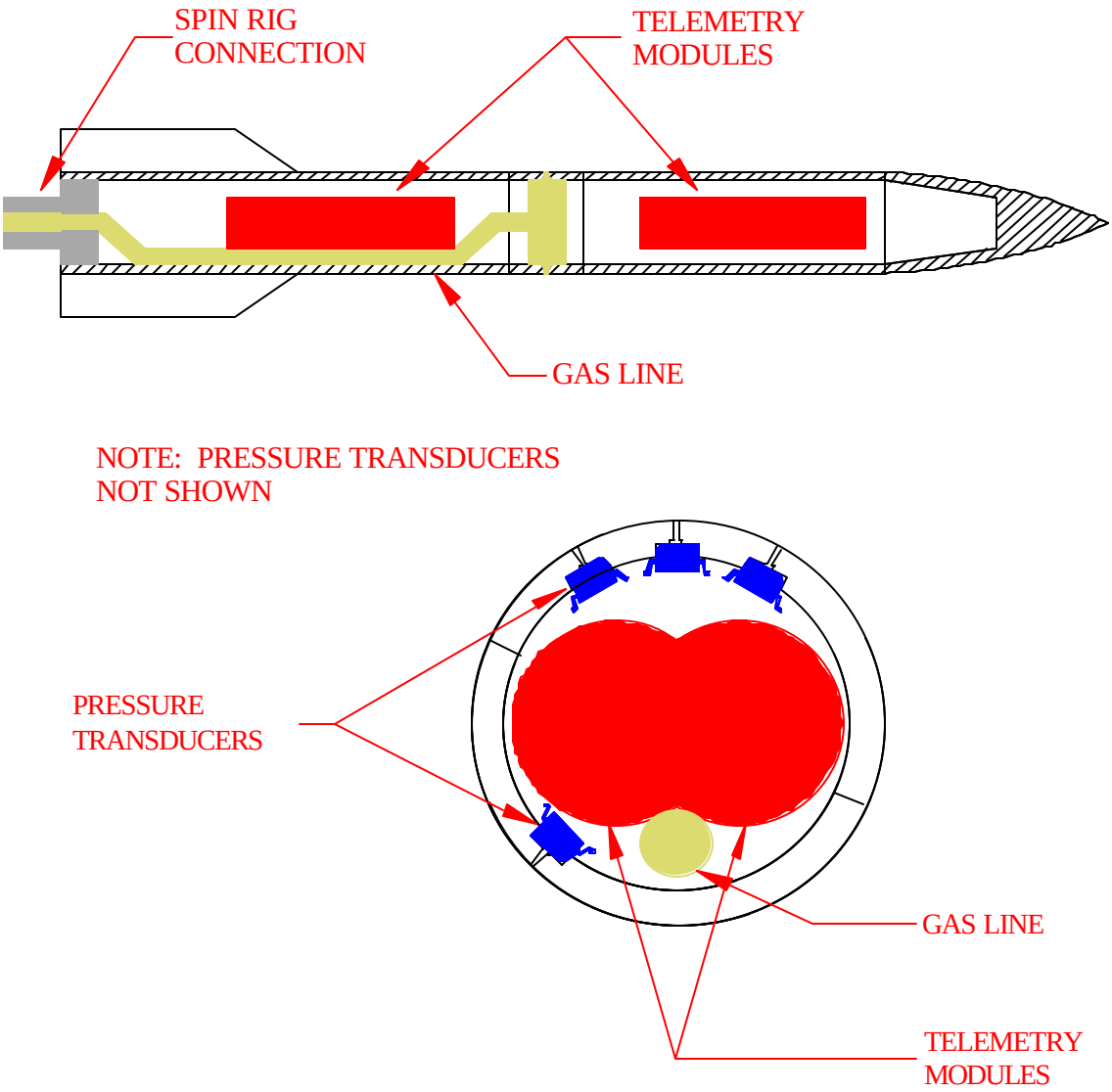

Figure 18 Conceptual cross-sections of the model showing telemetry and pressure transducer installation with a secondary gas line in place.

The fore, center, and aft segments all have the capacity to be positioned at different roll angles with respect to one another. This is to allow the single row of transducers in the fore segment to be aligned with any of the four rows of transducers in the aft segment. It also allows the jet nozzles to be clocked to different positions with respect to the transducers and the fins. This in particular is useful for the study of jet/fin interaction issues, because the location of the nozzles with respect to the fins is an important parameter. To accomplish this, the center segment is designed similar to a pipe union. The three segments are each clocked to the desired roll angle and held in position. Each end of the center segment is essentially a nut free to turn independently from the center of the segment where the nozzles are located. These "nuts" are then turned down on threads on the fore and aft segments until these segments are drawn into the center segment. Thus a variety of clocking positions are achievable.

In addition to the model itself, a new sting and a new spin rig were designed. These units attach to the rear of the model rather than at the model center of pressure to allow the internal space of the model to be used for instrumentation. Both the fixed sting and the spin rig must pass a pressurized gas across the junction to the model to supply the jets. For the fixed sting this is straightforward, but the spin rig must pass the gas across a rotating junction at 100 psi and 35 cfm. This is accomplished using a rotary seal. While it will increase the friction of the spin rig, the canted fins will still spin up the model even if the acceleration and steady-state angular velocity are not what they would be in flight. So long as the model rotates, meaningful jet/fin interaction studies can be conducted. The spin rig includes a Hall effect sensor as a means of recording the model's rotational behavior during a wind tunnel run. By employing magnets of various strengths to be used with the sensor, the unique rotational position of the sting can be determined at any given time, and then angular velocities and accelerations may be derived from that data. The spin rig also possesses a pneumatically-driven release pin to secure the model during wind tunnel startup, which can then be remotely released.

6.4 Assembly of the Wind Tunnel Model

The design and fabrication of the innovative wind tunnel model was performed by engineers and machinists at MicroCraft, Inc. of Tullahoma, Tennessee. The general design criteria were provided to MicroCraft by the authors and then the subsequent detailed design and fabrication process occurred over approximately six months. The pieces of the model, disassembled, are displayed in Figure 19 (neither the sting nor the spin rig is shown) and illustrate the composition as described above and the complexity of the wind tunnel model. All three jet sections are shown, though obviously only one may be used at any one time. A single set of four fins is displayed, as is the retaining ring that helps to hold them in place. No instrumentation has been installed in the model as illustrated in Figure 19.

Figure 19 Disassembled view of the innovative wind tunnel model.

The same parts of the wind tunnel model are shown fully assembled in Figure 20, except for the fin retaining ring (the rightmost piece found in Figure 19) because it must mount to the sting itself.

Figure 20 A fully assembled view of the innovative wind tunnel model, using the same parts shown in the photograph of Figure 19 (except for the fin retaining ring).

The spin rig is shown along with the fully assembled model in Figure 21. Alongside the model is one of the nozzle sections and the pressure tubing that connects it to the sting; this apparatus would be placed inside the aft segment of the model when operating the secondary gas supply to the jets simulating the spin rocket motors.

Figure 21 A view of the assembled model along with the spin rig, a nozzle section, and pressure tubing to supply the secondary gas supply to the jets.

A better view of the pressure transducer pockets can be seen in Figure 22, which shows one half of the aft segment of the model (Segment 1 in Figure 16). The foreground of the figure shows one of the NovaSensor pressure transducers that was installed into a recessed pocket using the epoxy method.

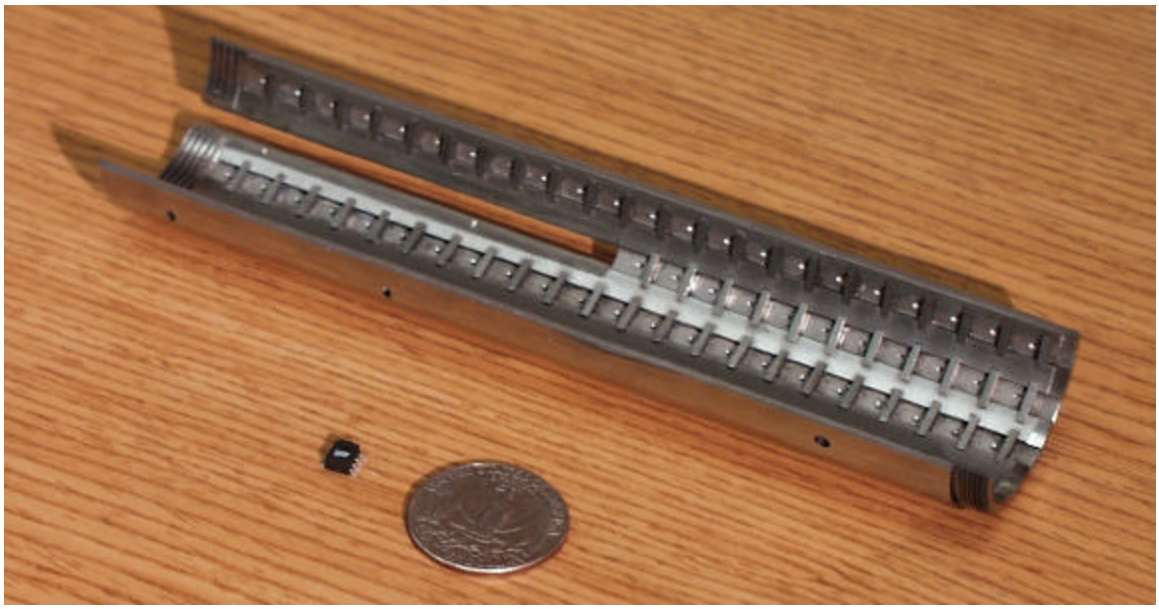

Figure 22 One-half of the aft segment of the model, showing the many pockets into which pressure transducers were installed. Shown in the foreground, alongside the quarter, is one of the NovaSensor pressure transducers that was installed into a pocket.

Model preparation began by selecting which transducer pockets would be used for the demonstration of the wind tunnel model's capabilities. Although there are 92 transducer pockets on the model, it is not feasible to install transducers in all of them for the simple reason that the wiring would require too much volume. Only 32 pressure transducer pockets were selected that covered different regions of the model as the locations that would be used. These transducers can be removed at a later date by using acetone to break down the epoxy holding them in place. Although it is likely that the NovaSensor transducers would be damaged in the process of removing the epoxy from the pockets, their low cost makes it practical to replace them. The Kulite transducers are not harmed by acetone (in fact, the manufacturer recommends the use of acetone to clean the transducer screens). For future experiments, transducers may be installed in those pockets most appropriate to that particular experiment; the present effort focuses on a demonstration of the experimental techniques and thus a few transducers in various locations is sufficient.

A total of 30 NovaSensor transducers and 2 Kulite transducers were selected for installation for the benchmark experiments. The NovaSensor transducers had either a pressure range of 0-15 psia or 0-30 psia depending upon where they were installed in the model. The larger pressure range was used for locations where stagnation effects were expected, such as upstream of the nozzles and upstream of the fins. The Kulite transducers were both sealed-gage transducers, sealed to sea-level atmospheric pressure with a range of +/- 2.5 psid.

The transducers were epoxied into the model using Devcon 2-ton Epoxy. This epoxy is fairly thin and flows well, which allows it to fill the narrow gap between the transducers and the pocket walls. The two Kulite transducers were epoxied into dummy modules shaped like the NovaSensor transducers, which were then installed as the others. Those transducer pockets not utilized were filled with wax to prevent air from flowing through the ports into the interior of the model. Once the transducers were secure, wires were carefully soldered to each lead. The soldering process for each transducer had to be rapid to avoid overheating each unit. Although 8 pins are present on each transducer, only 4 wires are needed; a positive voltage and a ground to power the transducer, and a positive and ground for the signal. Following the soldering process, a larger bead of epoxy was placed around the perimeter of the pocket and the junction with the side of the transducer. This was intended to provide an air-tight seal; any leak between the transducer pocket and the model interior would create a serious bias error. Finally, wires were bunched together and glued to the interior wall of the model using silicone.

Although the transducer installation and wiring procedure is easily described above, the actual process required several weeks of tedious labor. Included in this time was additional epoxying to seal transducers discovered to leak during a leak check procedure, repair of wires that did not adequately solder to the transducers, and a verification that each transducer continued to operate. Figures 23 and 24 show the model with the transducers installed for the forward segment and the half of the aft segment that contains the three rows of transducers, respectively.

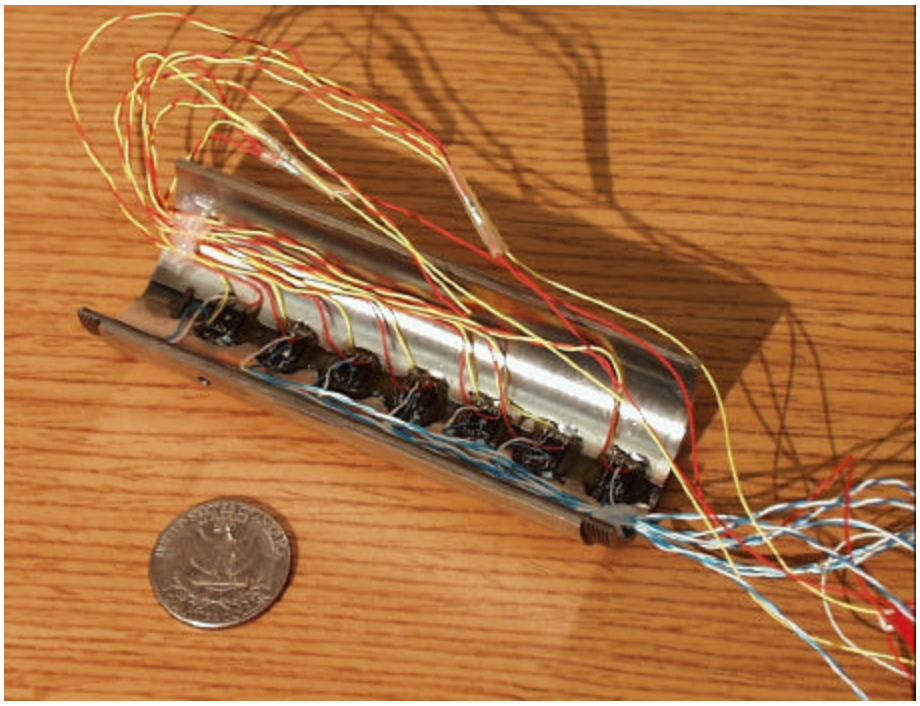

Figure 23 A view of one half of the forward section of the wind tunnel model following installation of the NovaSensor pressure transducers into the recessed pockets.

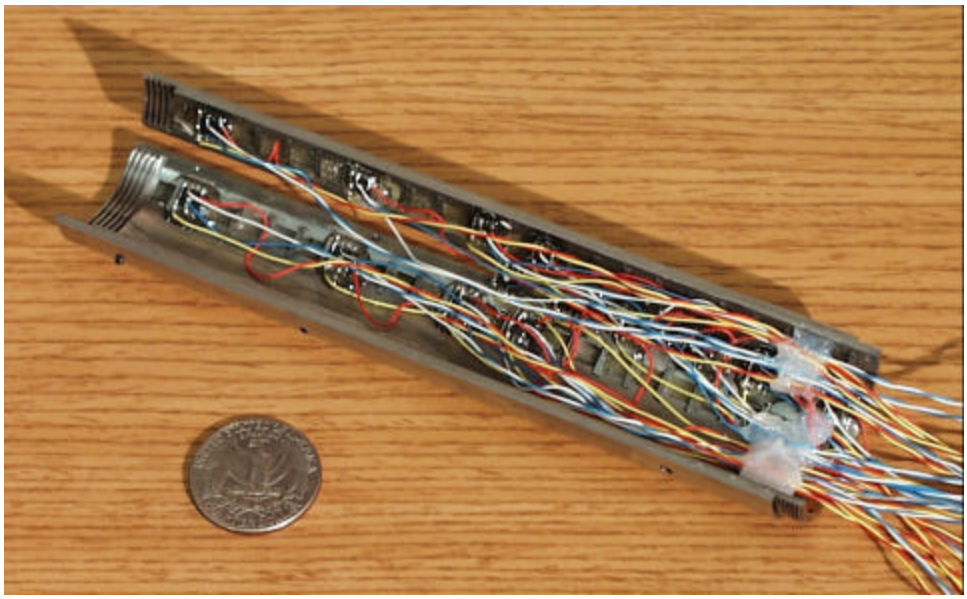

Figure 24 A view of one half of the aft section of the wind tunnel model following installation of the NovaSensor pressure transducers; this is the half section containing three rows of transducers.

Once the transducers were installed and verified to be performing nominally (using a calibration procedure in a pressure vessel), 16 of them were connected to one of the telemetry transmitters.

For the current demonstration, only one 16-channel transmitter was installed in the model. Although the wind tunnel model has been designed to contain three transmitters, such an installation will require a much more careful installation procedure using smaller, more delicate wire. Simplifying an already complex installation procedure was an important step towards successfully operating the experiment for the first time. Figure 25 shows the fore and aft segments of the model wired together through the hollow center section just prior to assembly. The two long black items are the transmitter and the battery. The many orange items are simply electrical tape wrapped around exposed wire where multiple connections were joined.

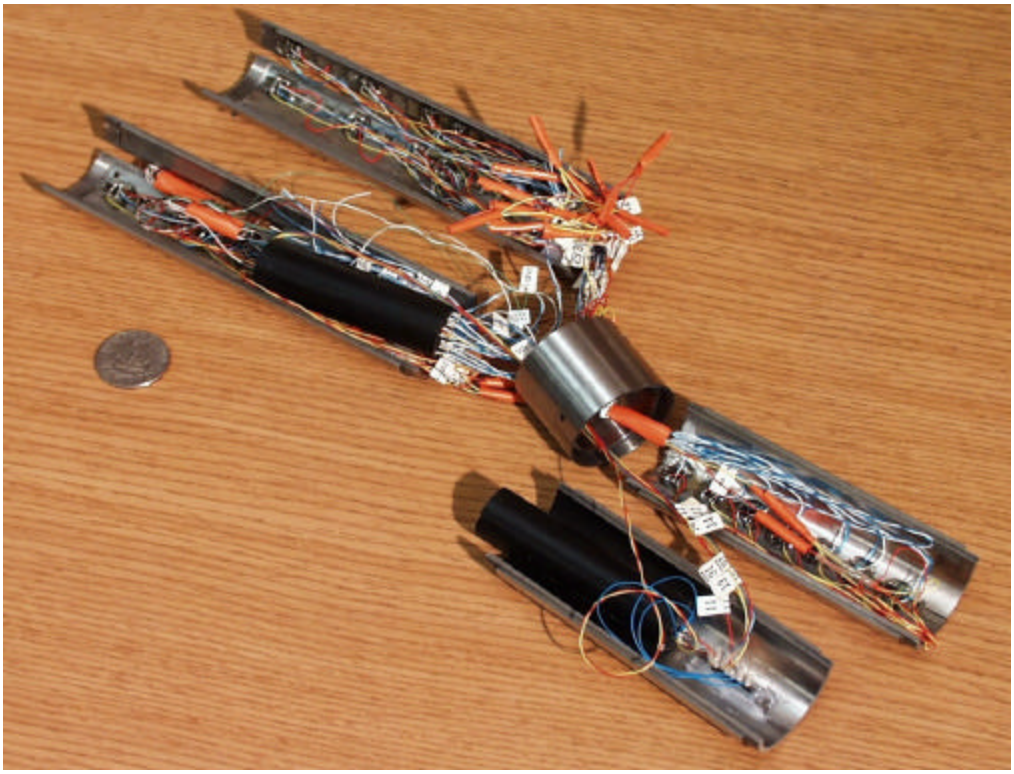

Figure 25 A view of the model wired just before full assembly; one transmitter and the battery are positioned in place.

Independent from the model assembly, the instrumented fin was sent to Kulite for the customized installation of the surface pressure transducers. Sealed-gage transducers, similar to the two installed into the model body, were placed in each of the 22 channels milled into the surface of the instrumented fin. The transducers themselves were covered with a hard RTV and the channels were filled with epoxy and flushed with the surface to ensure a flat face on each side of the fin. The wiring and temperature compensation modules protrude from the bottom of the fin, which would be located in the interior of the model where the transducers can be wired to the battery and the transmitter. A photograph of the completed instrumented fin is included as Figure 26.

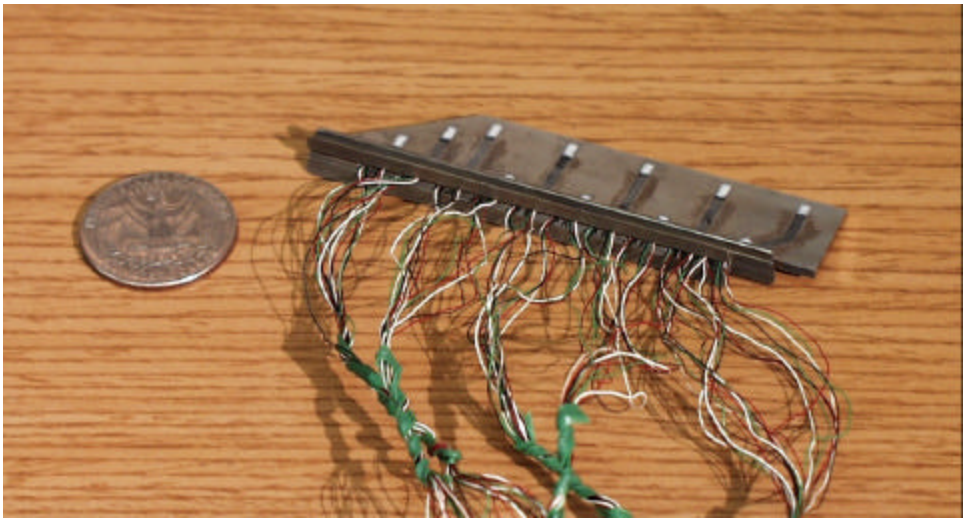

Figure 26 A photograph of the instrumented fin where the white squares are the RTV coatings protecting each transducer. There are 11 transducers located on each side.

Transmission of the signal was accomplished by protruding a small wire as an antenna from the base of the model, alongside the sting where it would not appreciably influence the flow over the model body. A receiving antenna was fashioned from coaxial cable and was placed on the outside of the porous wall test section but within the transonic plenum of the wind tunnel, then passed through the bulkhead of the plenum to be connected to the receiving electronics.

7. Experiments with the Innovative Model

While the innovative diagnostics LDRD effort was intended to get an early start on experiments in the program, the challenges involved with the sensors and data package significantly delayed hardware progress. As a consequence, experiments were conducted at the end of the program and were aimed at simply determining the viability of the designed systems.

A series of preliminary experiments was conducted in the TWT facility to examine the performance of the innovative model, the telemetry unit, the various pressure transducers, the onboard jets, and the spin rig in a shakedown mode of operation. These experiments were not intended to provide a comprehensive investigation of every detail of the system or a complete study of the flow physics present in jet-in-crossflow and jet/fin interactions. In particular, while basic uncertainties of the measurements were examined, a rigorous examination of potential bias errors that would be necessary for a validation experiment was beyond the scope of this project. Rather, the experiments conducted here at the conclusion of the LDRD program were designed to explore the utility and general system performance of the techniques and capabilities developed during this program and to demonstrate how they may be integrated into future research efforts.

Of the 32 pressure transducers that were installed and wired, 16 were connected to the single telemetry transmitter placed in the model. Of these, 15 produced useful data because one subsequently was found to be corrupt and could not easily be repaired. The locations of the 16 transducers are shown in the sketch in Figure 27. Transducer number 11 is the one that produced corrupt data. Transducers 10 and 17 are Kulite sealed gage transducers while the rest are NovaSensor transducers. All 16 channels were sampled at 12-bit at a bandwidth of 19.5 kbps, which worked out to a sampling rate of 886 samples/sec when overhead bits were considered.

The model was configured with the 15-minute fin cant set and the sonic nozzles were used to model the spin rocket jets. Even when operating in jet-off conditions, the nozzles remained in place to avoid the substantial difficulty of re-wiring the model. Furthermore, other crevices on the model surface, such as those for bolts and spanner wrenches, were not filled with wax to maintain a smooth surface contour. The model was configured in this manner because these experiments were intended to evaluate the performance of the model hardware, telemetry system, and pressure transducers and the measurement techniques rather than specifically examine the physics of finned axisymmetric bodies.

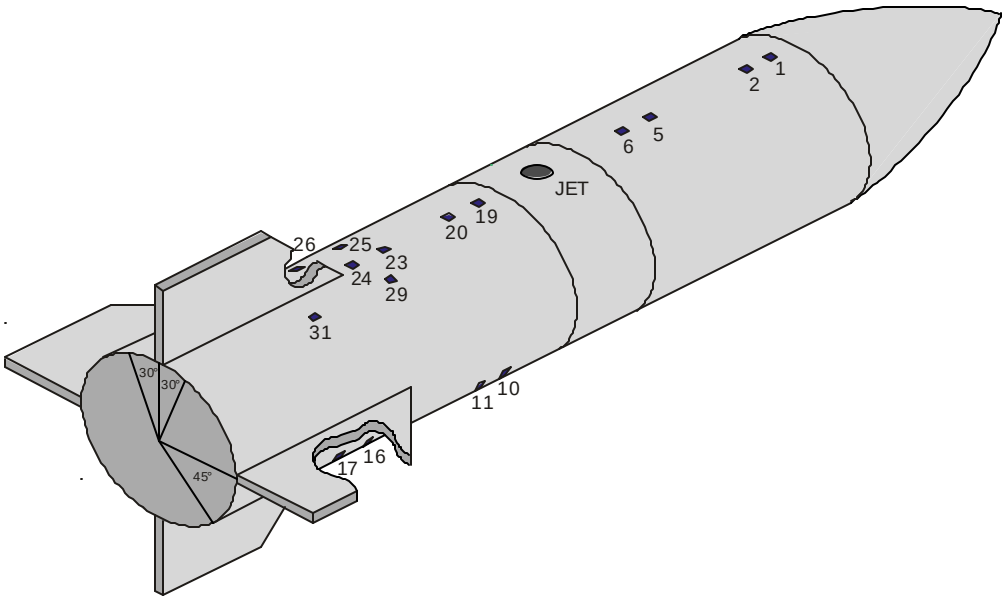

Figure 27 Sketch of the locations of the 16 pressure transducers that provided data from the model body. 32 transducers were installed, but only half used. Drawing not to scale.

The test conditions selected for all experiments had a freestream Mach number of M_8 =0.8 and stagnation pressure P_0=20.6 psia, which provided a freestream static pressure of p_w=13.6 psia. The value of M_8 was chosen because it is a condition commonly representative of transonic flight vehicles, and the value of p_w was chosen to create model pressures within the range of values most easily measured. Angle of attack varied and is noted as appropriate below, as is the stagnation pressure of the jet P_{0j}. Figure 28 shows the model mounted in the TWT's

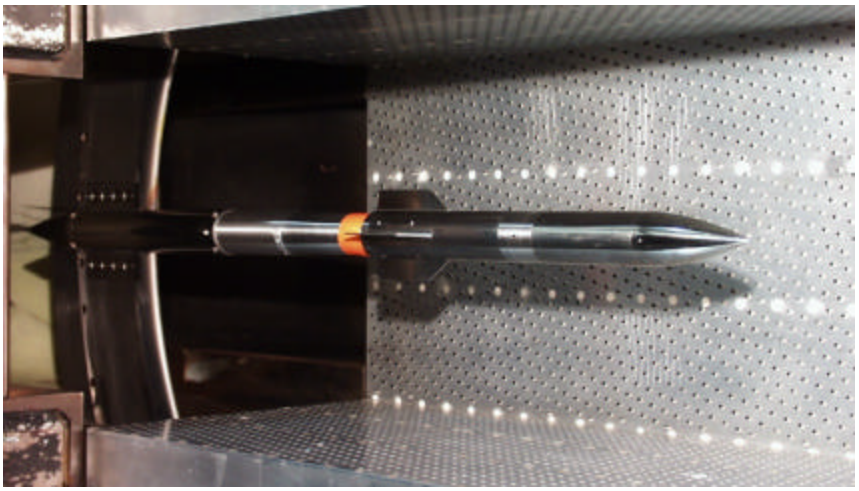

porous-wall test section on the new spin rig.

Figure 28 The innovative model mounted on the new spin rig located within the porous-wall test section of the TWT facility.

The initial experiments were conducted using the fixed sting with jet-off conditions. These were intended to evaluate the performance of the telemetry system and the validity of the transmitted data as well as to provide a fixed reference frame comparison to the spinning body data that would follow. Several runs were conducted at zero angle of attack (a=0°) with the jets off to assess the repeatability of the measurements. The results are shown in Figure 29. The typical uncertainty bars that are shown were derived from repeated instrumentation calibrations and represent the precision uncertainty but not possible biases. As can be seen, the repeatability of

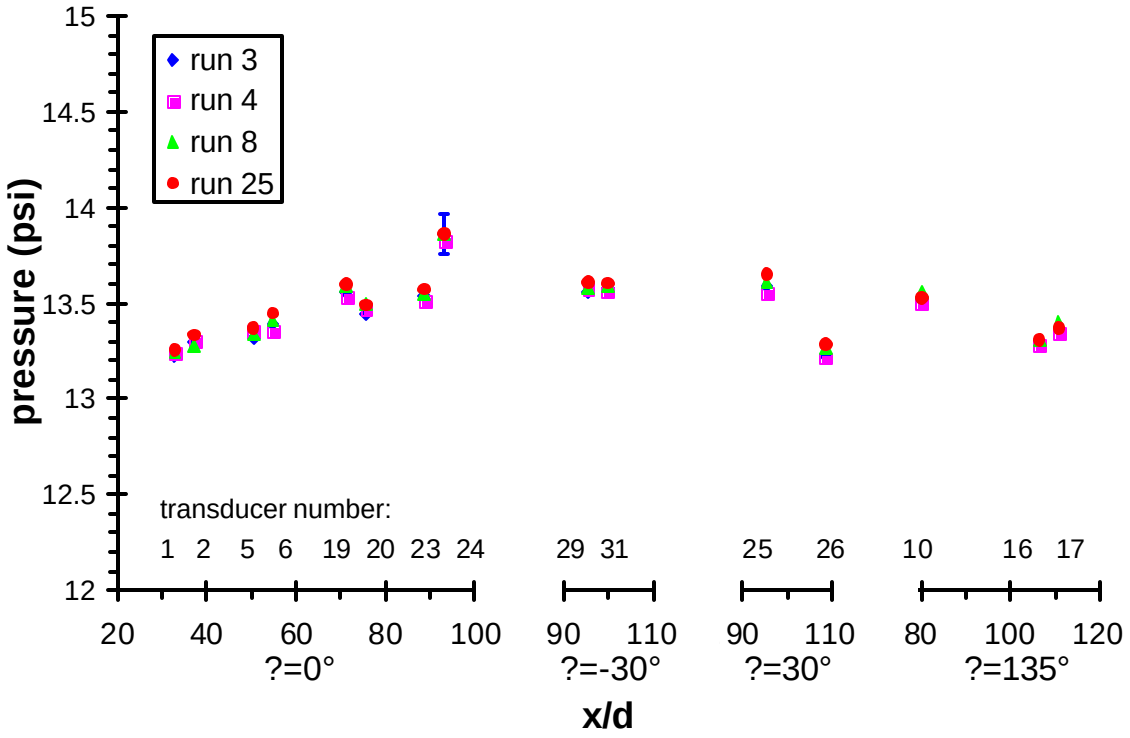

each transducer is well within the precision uncertainty.

Figure 29 Surface pressure data for a=0°, jets off, showing four wind tunnel runs for repeatability characteristics. A typical data uncertainty is shown as well.

Experiments were then conducted on the fixed sting with the jets operational at different pressures to determine if the jet-in-crossflow effects produced would be detectable by the pressure transducers. Figure 30 shows the variation of surface pressures as the jet stagnation pressure is increased. The vast body of jet-in-crossflow research [10], as well as several studies specific to jets in transonic crossflow [11-16], has shown that within a few jet exit diameters of the jet, a change in surface pressure can be expected. In general, the pressure

increases upstream of the jet as the freestream stagnates against the jet plume, while the pressure decreases in the jet's wake. In Figure 30, it is evident that the effect of the jet exceeds the data uncertainty only on the three transducers closest to the jet, all of which are within approximately 10 jet diameters. Transducers further away detect no significant pressure change. This is consistent with past research showing that the effect of the jet on surface pressures is clear only in the near field, which can be considered to extend to about 10 jet

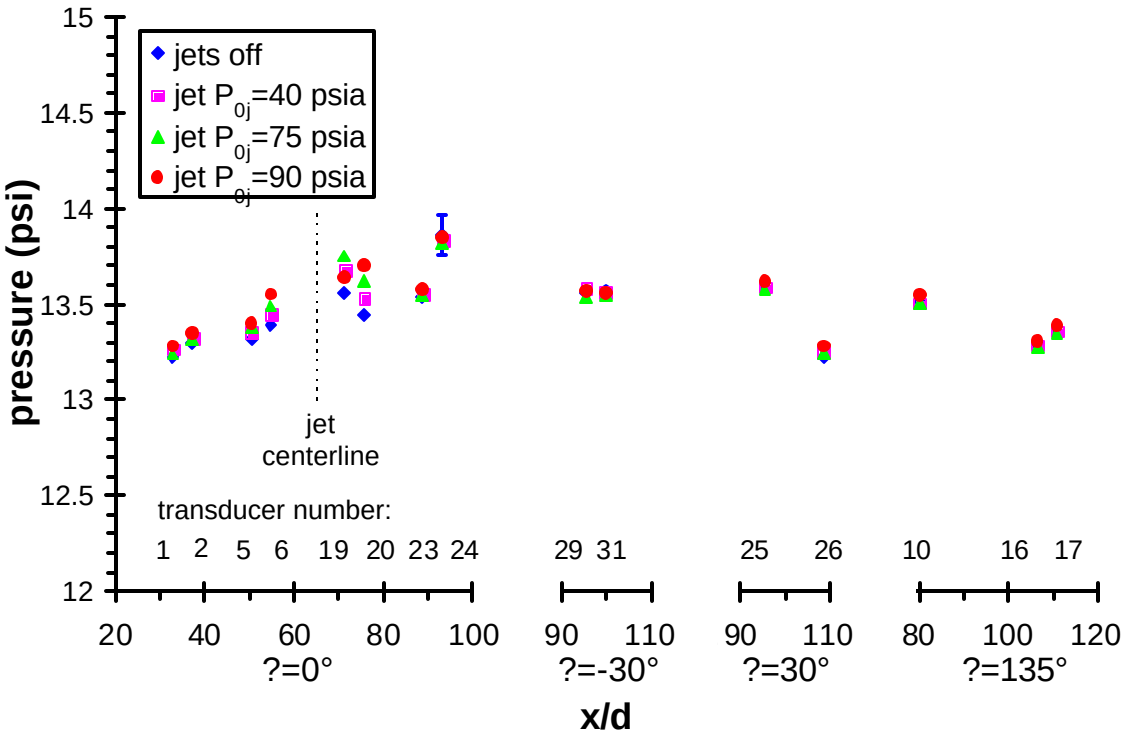

diameters and not much further. The surface pressure does increase as expected upstream of the jet as the jet stagnation pressure is raised, but the surface pressures in the jet's wake also increase with jet pressure. No reason for the latter behavior is apparent.

Figure 30 Surface pressure data as jet stagnation pressure is increased for α=0.

Additional pressure measurements were gathered with the model pitched to a positive angle of attack. This placed those transducers mounted at a roll angle of 0° directly in the leeward side of the model. Figure 31 shows the results. Wind tunnel runs were conducted for a=0, 5, and 10° with the jets off and at a=10° for the jets on at a stagnation pressure of 90 psia. A 10° angle of attack probably will not experience interference from the wind tunnel walls, even for such a large wind tunnel model. Larger pitch angles were not tested because of the tunnel blockage issues that would arise and the much larger loads placed on the model. This is one of the limitations of an increased model size.

The pressure variations due to the pitch angle in Figure 31 are substantially larger than those simply due to jet pressure. It appears that the effect of the jet is enhanced at angle of attack as compared to zero angle of attack; however, it seems unlikely that the jet's influence would be felt near the nose of the model (transducer 1) or near the fins (transducers 17 and 26, for example). It may be that some shift in the data resulted from an unexplained instrumentation event. Additional runs were conducted with the roll angle of the model shifted from 0° in Figure 31 to 90, 180, and 270°, but this data is not shown here (some of it can be seen in later

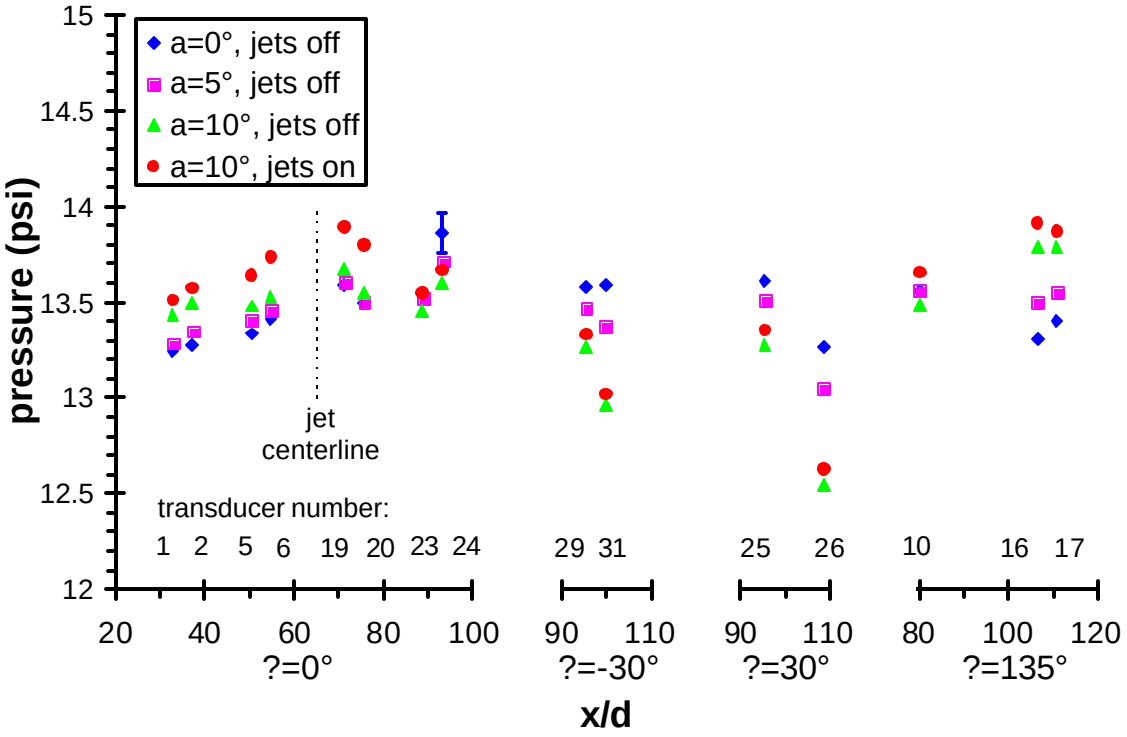

figures). These roll angles placed the transducers and the jets into different positions relative to the model pitch direction and become important when investigating the pressures measured while the model rotates as discussed in the section below.

Figure 31 Surface pressure data as the model is pitched to angle of attack, including one run with the jets on at a stagnation pressure of 90 psia.

Figures 29 through 31 demonstrate that the instrumentation techniques and innovative model design developed within this project have been successful at producing data for jets-on and jets-off conditions and for different angles of attack, although further experiments are needed to fully understand the quality of the pressure data. Continuing the experimental program, the fixed sting was removed from the wind tunnel and replaced with the new spin rig. The Hall effect sensor was tested and aligned to the zero roll angle of the model. For jets-off conditions, the rotary seal for the gas supply line was removed from the spin rig to reduce the friction. A

noticeable difference in the spin rig's rotational properties was observed when the seal was removed. Because of the additional rotational friction that limited the roll rate of the model, the 15-minute fin cant was replaced with 30-minute fin cant to generate larger torque and hence produce a larger roll rate.

The first experiments conducted on the spin rig were run at zero angle of attack with the jets off. Although no angular variation in the surface pressure was expected (or found), this provided an opportunity to compare the mean pressures during rotation with those acquired on the fixed sting. Pressures matched to within approximately 0.1 psi, which is within the precision uncertainty of the measurements. It was found that the pressures from the NovaSensor transducers were affected by temperature as the model heated at the beginning of the wind tunnel run, but the Kulite transducers were uninfluenced because they have temperature compensation. When the wind tunnel was run for a short duration prior to data acquisition, consistent results and a good match with the fixed sting data was achieved.

Data were acquired with the model spinning and the jets off for pitch angles of a=5° and a=10°, then phase-averaged in 10° increments to produce a representative pressure trace around the perimeter of the model as it rotates. The results are shown for three sample transducers in Figures 32 and 33 for a=5° and a=10°, respectively; other transducers display similar results. Transducer 1 is located near the nose of the model, transducer 24 is located just upstream of one of the fins, and transducer 16 is located between two fins. The figures also show the pressures recorded on the fixed sting for roll angles in increments of 90°, which maintains the symmetry of the model with respect to the pitching direction. The fixed-sting data for transducer 16 is shifted by 45° from the other two transducers because that transducer is not located along the same line of pressure taps.

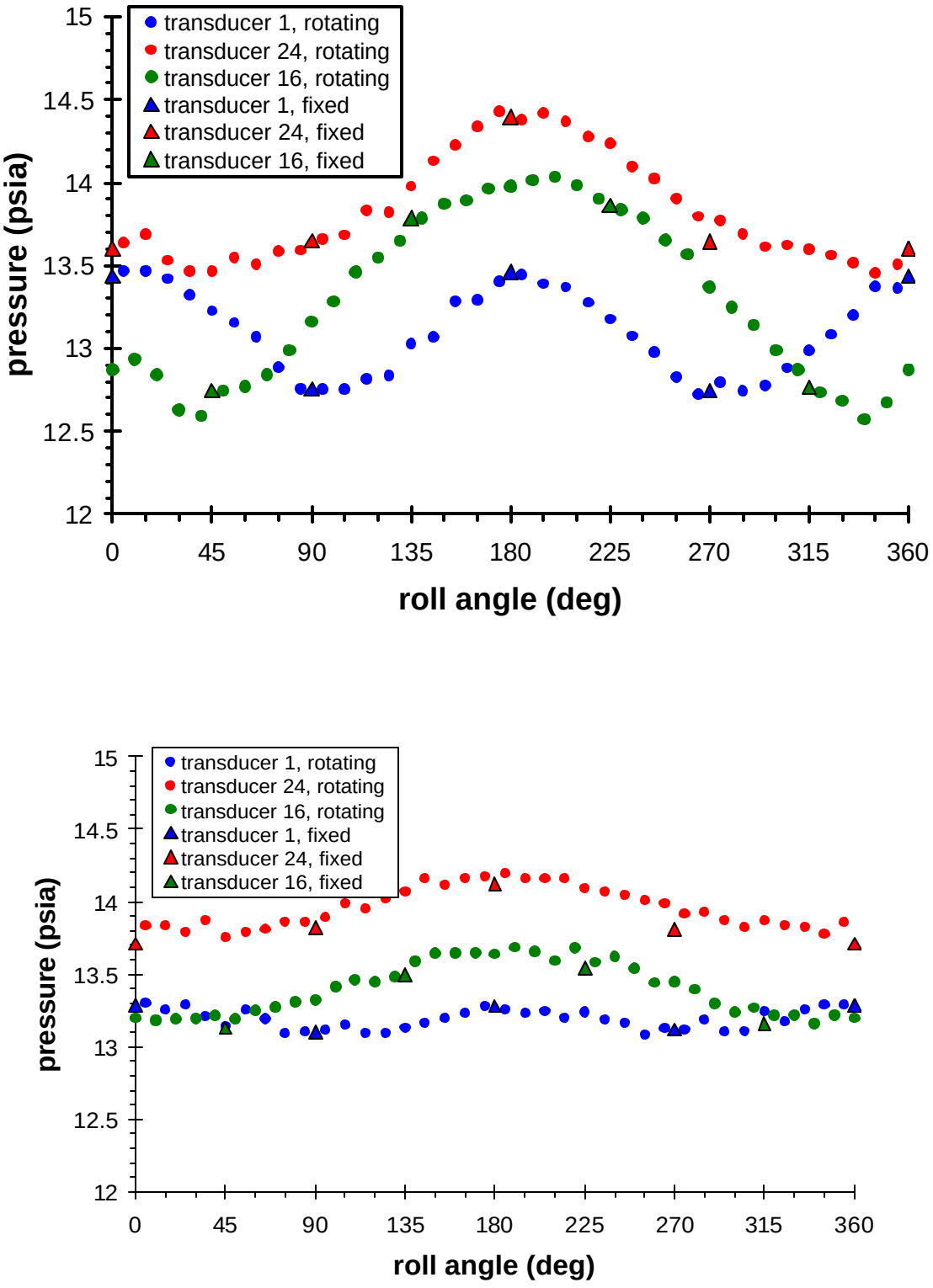

Figure 32 Phase-averaged surface pressure data from three sample transducers with the model pitched to an angle of attack of a=5° and with the jets off.

Figure 33 Phase-averaged surface pressure data from three sample transducers with the model pitched to an angle of attack of a=10° and with the jets off.

Two particularly interesting features may be discerned from Figures 32 and 33. Transducer 24, located at the fin leading edge where the flow will stagnate, shows a high pressure on the windward side (180°) and a low pressure on the leeward side (0°), which is the expected behavior. On the other hand, transducer 1, located near the model's nose, shows approximately equal high pressures at both the windward and leeward sides (0 and 180°) with low pressures midway between these two points (90 and 270°). This is counter-intuitive and may indicate the presence of a separation and subsequent reattachment region on the leeward side of the model. There is insufficient data to determine this. Transducer 16, located midway between two fins, is somewhat a combination of the previous two pressure traces. The highest pressures are found on the windward side, but the lowest pressures are about 45° removed from the leeward position. Presumably this results from the influence of the fins.

Also clear from Figures 32 and 33 is that the fixed-sting pressures are, to within the various uncertainties of the measurements, a match with the rotating pressures. If the model is manually rolled between wind tunnel runs, the same data will be produced as for a rotating model. This is not surprising, since the current model rotation rates did not exceed 5 Hz. At these rates, the freestream velocity is much larger than the rotational velocity and any spinning-body physics appear negligible. However, higher rotation rates may induce additional effects that require the use of spinning models to obtain useful data.

A few wind tunnel runs were conducted with the jets on and the model rotating. This was intended primarily to demonstrate that the jets could be operated simultaneous with model rotation, but the presence of the additional friction created difficulties spinning the model. Rotation rates of about 1 Hz represented the apparent limit. However, meaningful data was acquired showing the effects of the jet, but to achieve sufficient roll rate in future experiments, either larger fin cant or some sort of motorized sting will be necessary. Figure 34 shows representative data with the jets operating at a stagnation pressure of 90 psia at a pitch angle of 10°. Sample data from the three transducers nearest the jet are shown, since previous data has indicated that transducers further from the jet will not detect its influence. Transducer 6 is upstream of the jet and transducers 19 and 20 are downstream of it. Agreement with the fixed-sting data is not as good as seen in Figures 32 and 33, particularly for transducer 19, but it is unclear if this is an instrumentation issue or a physical issue. For comparison, Figure 35 displays data from the same three transducers at a=10° but with the jets off.

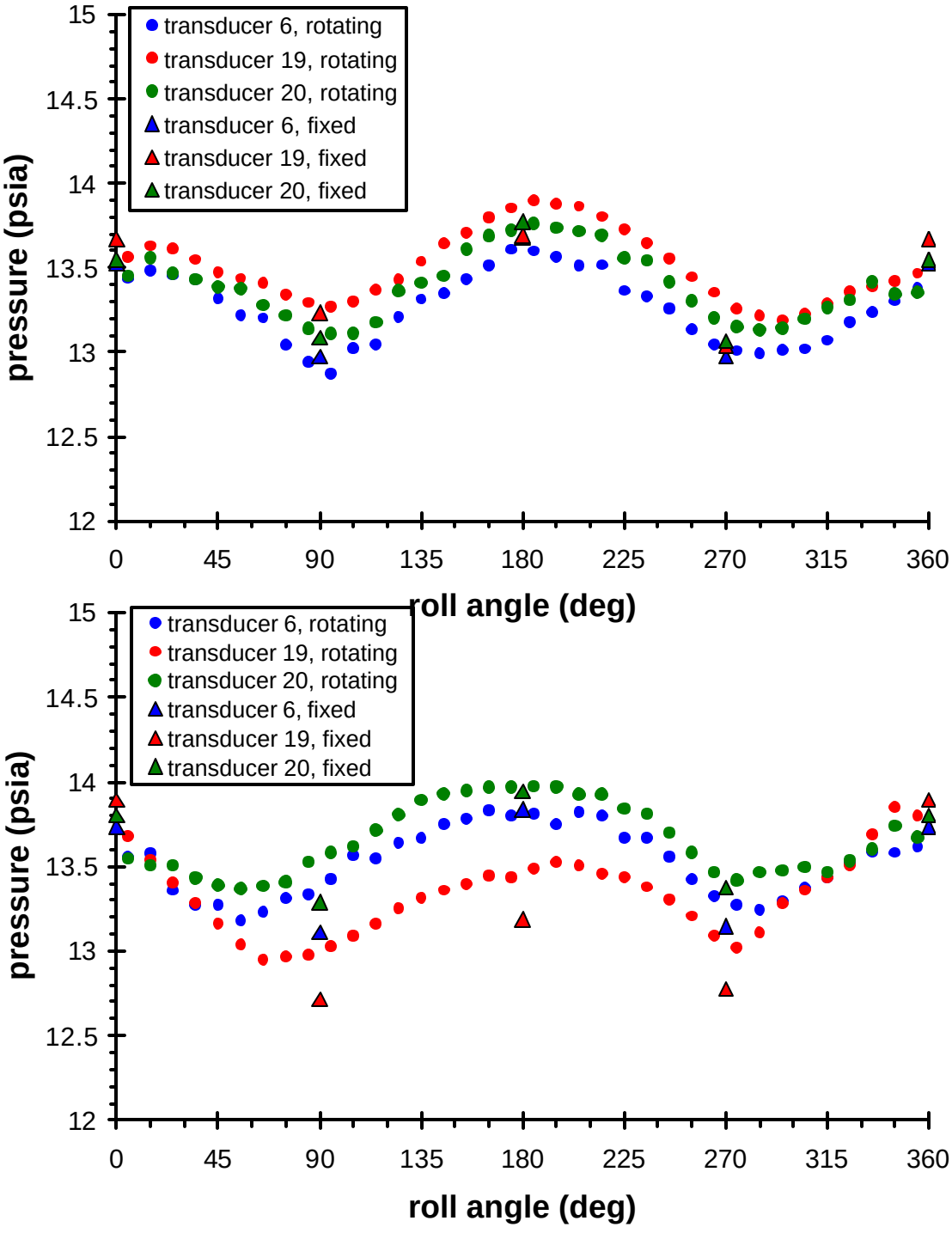

Figure 34 Phase-averaged surface pressure data from the three transducers closest to the jet with the model pitched to an angle of attack of a=10° and the jets operating at 90 psia.

Figure 35 Phase-averaged surface pressure data from the three transducers closest to the jet with the model pitched to an angle of attack of a=10° but the jets off.

Following the use of the model body pressure transducers, the model was disassembled and rewired for experiments utilizing the instrumented fin. The instrumented fin contains 11 transducers on each side. Because of the finite thickness of the fin, transducers could not be placed directly opposite each other. Instead, they are staggered such that every other transducer is located on each side of the fin. Transducers instrument the leading edge of the fin, then form two rows along its length, one near the top of the fin and one near its root. This is sketched in Figure 36. The 14 transducers nearest the fin's leading edge plus the two rearmost transducers were connected to the telemetry transmitter. Transducer 6 failed early in the experiment and could not be revived. As with the model body transducers, all channels were sampled at 12 bits and 886 samples/sec.

The model was moved back to the fixed sting and the 15-minute cant fin set was re-installed. Initially, the jets were aligned to the same roll angle as the instrumented fin. Data were acquired for jets-off conditions and then for four different jet stagnation pressures; Figure 37 shows the results. The pressures acquired near the leading edge of the fin show a gradual decrease from

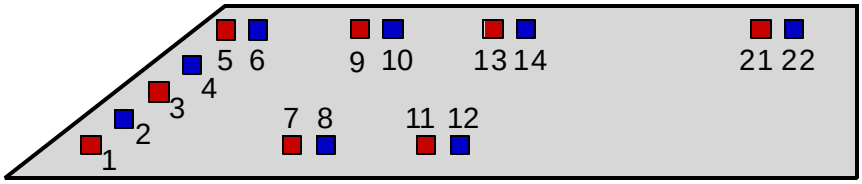

the fin root to its tip, with no clear difference from one surface of the fin to the other. Once the jets are turned on, it is clear that the effects of the jet are seen only near the leading edge of the fin; further along its length, no discernable change in pressure is observed. Further runs were conducted where the roll position of the nozzle with respect to the fin was shifted in 10° increments to assess the influence of the nozzle clocking position on the fin pressures, with the jet shifted to the leeward side of the fin cant. Figure 38 shows the fin pressures with the nozzle clocked to 20°. Here, the pressure difference across the fin is clear.

Figure 36: Locations of the 16 transducers that provided data from the fin, of the 22 that were installed. Locations in red are on the side of the fin nearest the jet as the jet is clocked to different angles with respect to the fin, and locations in blue are on the far side.

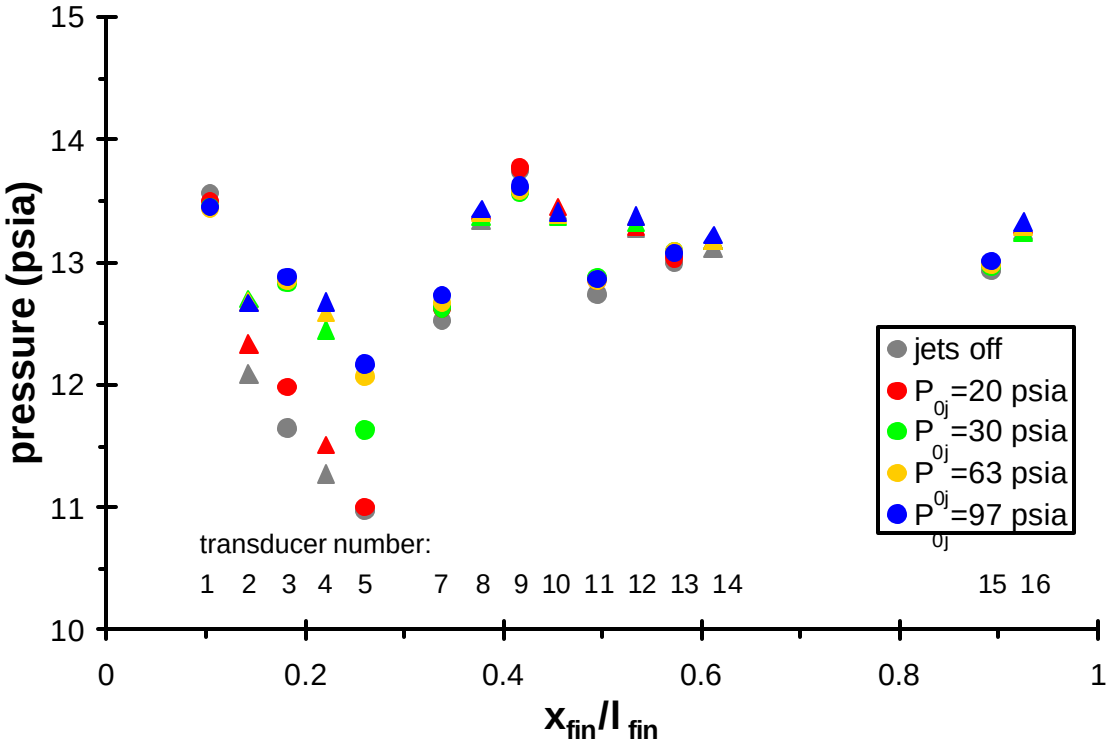

Figure 37: Fin pressures as jet stagnation pressure is varied with the jet nozzle aligned with the fin. Circular data points are on the side of the fin nearest the jet as the jet is clocked to different angles with respect to the fin; triangular points are on the far side.

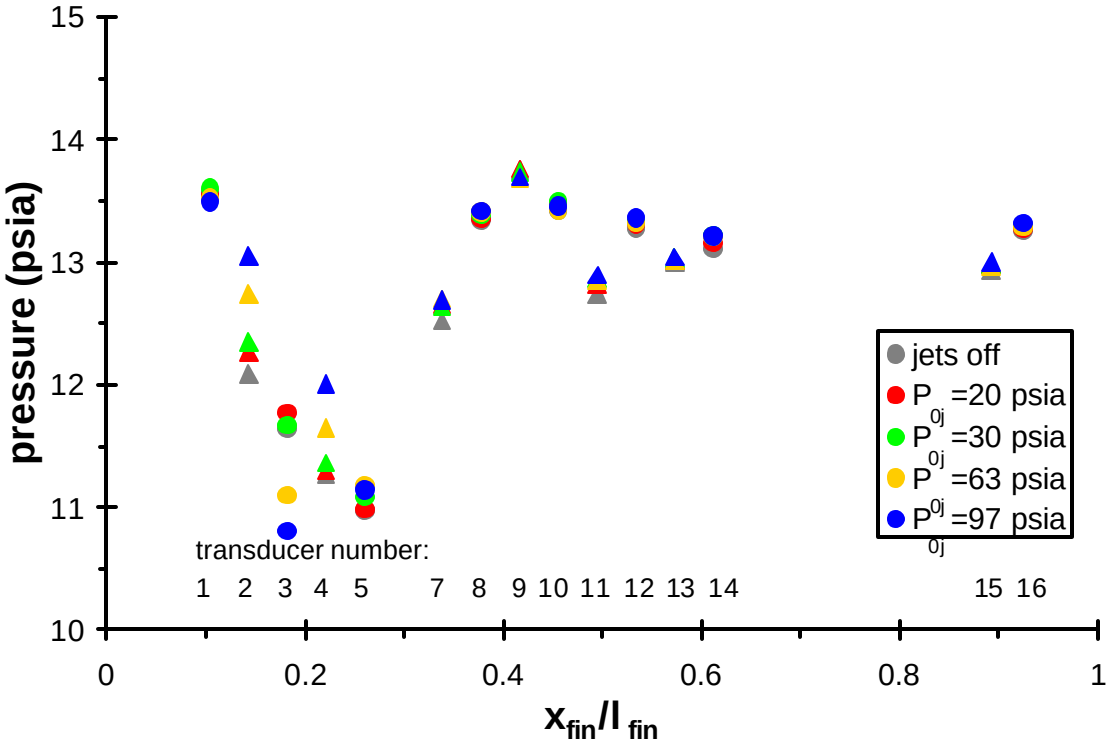

Figure 38: Fin surface pressures as the jet stagnation pressure is varied with the jet nozzle 20° from the fin. Circular data points are on the side of the fin nearest the jet as the jet is clocked to different angles with respect to the fin, and triangular data points are on the fin's far side.

Only four transducers, all of which are located along the leading edge of the fin, show a significant variation due to the presence of the jet. To determine a representative pressure difference across the fin, the average pressure of the two of these transducers on the fin surface nearest the jet were subtracted from the average pressure of the two transducers on the fin surface furthest from the jet. Since the transducers on each side of the fin are not directly opposite each other, a positive pressure difference is formed even when the jet is not operational. This bias was computed from the jets-off case and subtracted from the jets-on pressure differences to create a quantity $(?p)_{fin}$ that represents the effect of the jet on the fin. While this is not the true pressure difference across the entire surface area of the fin, it is a convenient value that can be used to track trends influencing the fin pressures.

Figure 39 shows the influence of the nozzle clocking position on $(?p)_{fin}$. Because the nozzle segment of the model was not geared for specific angles, the nozzle position was accurate only to within about ±2°. This is probably a factor in $(?p)_{fin}$ reaching zero at about 3° rather than 0°, although nozzle asymmetries and the fin cant may be additional causes. At any rate, Figure 39 demonstrates that when the jet is aligned to the fin, the effect on the fin pressure is relatively equal on each surface, which is logical given the symmetry of the model and flowfield. As the nozzle is shifted to one side of the fin, the effect on the fin becomes pronounced, reaches a peak near 20°, then gradually diminishes as the jet is distanced from the fin.

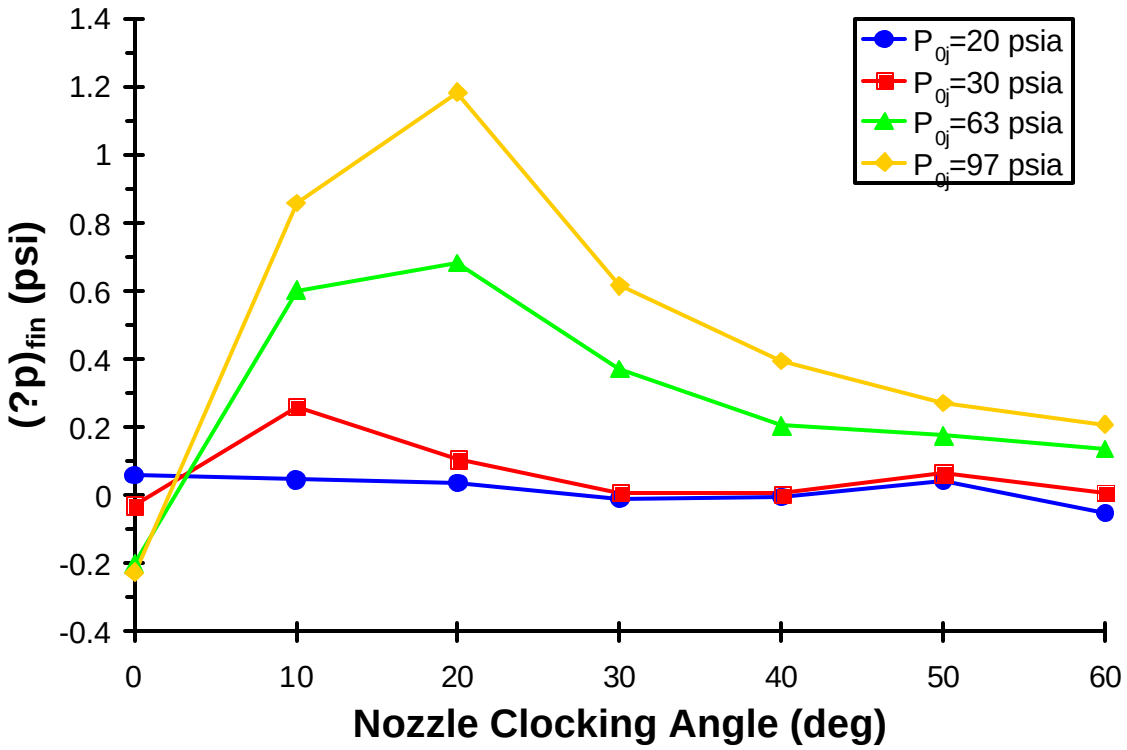

Figure 39: Variation in representative pressure differential across the fin $(?p)_{fin}$ as the nozzle clocking position is varied with respect to the fin position.

Additional wind tunnel runs were conducted to examine the influence of the model pitching angle on the fin pressures. These are shown in Figure 40. The jet stagnation pressure was maintained at 97 psia for all conditions. As the jet nozzle was clocked to different alignment angles with respect to the instrumented fin, the fin remained in the 0° roll position with respect to the model pitch direction. As the figure shows, the peak value of the pressure differential across the fin shifts to a different nozzle clocking angle as the angle of attack changes. This demonstrates that the influence of the jet upon the fin pressures varies not just with the relative position between the nozzle and fin, but also with the attitude of the vehicle itself.

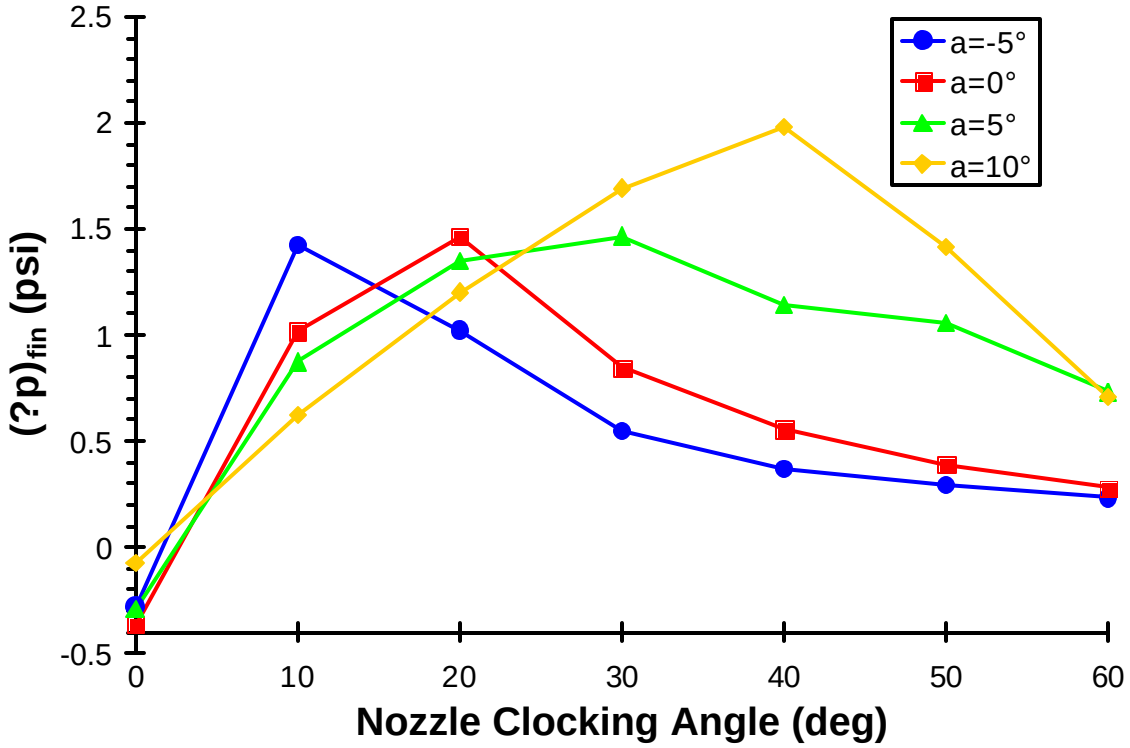

Figure 40: Variation in representative pressure differential across the fin $(?p)_{fin}$ as the nozzle clocking position is varied with respect to the fin position and the angle of attack of the model is altered. The jet stagnation pressure is 97 psia for all cases.

8. Conclusions

The innovative diagnostics LDRD program was successful in a wide variety of areas and provided an intensive learning effort for scale model experiments in the TWT facility. The parallel development of a data acquisition and telemetry system with a brand new model proved challenging and complex. The movement forward of a technology capability for our use in the wind tunnels was costly and driven by the difficulties of scale. However, the following conclusions can be drawn:

- A miniaturized data acquisition and telemetry system has been developed and tested for acquisition of multiple channels of data on a model as small in diameter as 1.5 inches in the TWT facility.
- A new and innovative model has been designed, fabricated, and used in the wind tunnel for research into jet/fin interactions. The model has valuable flexibility in design and greatly extends the types and number of measurements able to be made in Sandia's facilities, including the operation of very small onboard jets for the simulation of spin rocket motors. In addition, the model incorporates the ability to traverse a gas across a rotating junction.
- Data telemetry hardware and software have been acquired from SRI, Inc. and a number of systems have been used to gain experience with transmission of acquired data within the TWT facility. This represents a giant step forward in terms of a new method of data acquisition from small-scale models at Sandia.
- A capability has been developed to place microsensor instrumentation for pressure measurements on the body of a wind tunnel model and on both sides of a fin as thin as 0.063 inch.
- The difficulties of making measurements for complex fluid interactions in a small wind tunnel with a small model have been determined, and methodologies have been examined to maximize the potential for successful data acquisition under these conditions.
- A new method of spinning models in the TWT facility has been designed and fabricated, adding capability to the existing and traditional spin rig. The mechanism is enhanced using a Hall effect sensor for not only determining spin rate but also angular position.
- Experimental evidence of the effects of jet/fin interaction on the pressure distribution on one of the model fins was observed using the new experimental capabilities developed through this program.
- The new hardware capabilities used during the LDRD project will be available for future experiments for gravity bomb type geometries.

9. Recommendations

Based on the experiences during this LDRD research program and as a consequence of the results of the model experiments, a number of recommendations can be made for future work in the area of diagnostics development. In particular, further work is required on the telemetry systems development, the application of microsensors for wind tunnel measurements of pressure, and model rotation techniques. Thus, based on the work in this LDRD program, the following efforts are recommended:

- Further experiments are required to examine pressure trends for non-zero angle of attack configurations where significant pressure differences occur.
- Better packaging of pressure microsensors is required to attain higher spatial resolution along the axis of the wind tunnel model.
- Further investigation of methodologies for transfer of the secondary gas supply across a moving boundary might improve the achievable rotation rate.
- Temperature compensation circuitry for all pressure microsensors would eliminate a source of bias error in the pressure data and afford more flexibility in long wind tunnel operations.
- Integration of optical diagnostics into the analysis of the jet/fin interaction problem should be a long-term goal.
- Further experiments are warranted for understanding of some of the pressure interaction trends evidenced in the data in this report.
- Further research into the acquisition of pressure microsensors with higher performance standards is warranted as well.

10. References

1. Eaton, W. and Smith, W., "Micromachined Pressure Sensors: Review & Recent Developments," Smart Materials and Structures, Vol. 6, No. 5, October 1997, pp. 530-539.

2. Lofdahl, et al., "Small Silicon Pressure Transducers for the Space-Time Correlation Measurements in a Flat Plate Boundary Layer," **FED-Vol. 197**, *Application of Microfabrication to Fluid Mechanics*, ASME 1994, pp. 25-30.

3. S. Ansermet, et al., "Cooperative development of a piezoresistive pressure sensor with integrated signal conditioning for automotive and industrial applications," *Sensors and Actuators*, **A21-A23**, pp. 79-83.

4. Trott, W. M., Wong, C. C., Longcope, D. B., Castaneda, J. N., and Amatucci, V. A., "Evaluation of Surface-Micromachined Pressure Sensors for Dynamic Pressure Applications," FEDSM'01-18213, Proceedings of the 2001 ASME Fluids Engineering Division Summer Meeting, New Orleans, Louisiana, May 29 – June 1, 2001.

5. Amatucci, V. A., Cole, J. K., and Hailey, C. E., "Air Dropped Surface Craft Scale-Model Water Entry Experiments," SAND91-2242, Sandia National Laboratories, Albuquerque, New Mexico, October 1991.

6. Iga, et al., Fundamentals of Microoptics: Distributed Index, Microlens, and Stacked Planar Optics, Academic Press, New York, 1984.

7. Valette, et al., "Silicon-based Integrated Optic Technologies," *Solid State Technology*, February 1989, pp. 69-75.

8. Liu, et al., "MEMS for Pressure Distribution Studies of Gaseous Flows in Microchannels," Proceedings of the IEEE on Micro Electro Mechanical Systems, 1995.

9. Goldstein, Richard J., Fluid Mechanics Measurements, Second Edition, Taylor & Francis, Washington, D.C., 1996.

10. Chinnock, et al., "Flow Visualization of Radial and Inline Jet Impingement," **FED-Vol. 172**, *Experimental and Numerical Flow Visualization*, ASME 1993, pp. 19-27.

11. Beresh, S. J., Henfling, J. F., and Erven, R. J., "Surface Measurements of a Supersonic Jet in Subsonic Compressible Crossflow," AIAA Paper 2001-2786, June 2001.

12. Chocinski, D., Leblanc, R., and Hachemin, J.-V., "Experimental/Computational Investigation of Supersonic Jet in Subsonic Compressible Crossflow," AIAA Paper 97-0714, January 1997.

13. Lee, E. E. Jr, and Willis, C. M., "Interaction Effects of a Control Jet Exhausting Radially from the Nose of an Ogive-Cylinder Body at Transonic Speeds," NASA TN D-3752, January 1967.

14. Manela, J., and Seginer, A., "Interaction of Multiple Supersonic Jets with a Transonic Flowfield," AIAA Journal, Vol. 24, No. 3, 1986, pp. 418-423.

15. Reichenau, D. E. A., "Interference Effects Produced by a Cold Jet Issuing Normal to the Airstream from a Flat Plate," AEDC TR-67-220, October 1967.

16. Shaw, C. S., and Margason, R. J., "An Experimental Investigation of a Highly Underexpanded Sonic Jet Ejecting from a Flat Plate into a Subsonic Crossflow," NASA TN D-7314, December 1973.

Distribution

MS 0188	1030	C. E. Meyers
MS 0188	1030	LDRD Office File
MS 0429	2100	J. S. Rottler
MS 0447	2111	J. O. Harrison
MS 0447	2111	P. D. Hoover
MS 0634	2951	K. V. Chavez
MS 0841	9100	T. C. Bickel
MS 0841	9100	C. W. Peterson
MS 0824	9110	A. C. Ratzel
MS 0834	9112	M. R. Prairie
MS 0834	9112	V. A. Amatucci (25 copies)
MS 0834	9112	S. J. Beresh (5 copies)
MS 0834	9112	C. J. Bourdon
MS 0834	9112	J. F. Henfling
MS 0834	9112	R. J. Erven
MS 0826	9113	W. L. Hermina
MS 0834	9114	J. E. Johannes
MS 0825	9115	W. H. Rutledge
MS 0825	9115	D. W. Kuntz
MS 0825	9115	W. P. Wolfe
MS 0836	9116	E. S. Hertel
MS 0836	9117	R. O. Griffith
MS 0847	9120	H. S. Morgan
MS 0824	9130	J. L. Moya
MS 0835	9140	J. M. McGlaun
MS 9018	8945-1	Central Technical Files
MS 0899	9616	Technical Library (2 copies)
MS 0612	9612	Review & Approval Desk For DOE/OSTI